Aspergillus fumigatus can display persistence to the fungicidal drug voriconazole

Jennifer Scott[1#], Clara Valero[1,2#], Álvaro Mato-López[3], Ian J. Donaldson[4], Alejandra Roldán[3], Harry Chown[1], Norman Van-Rhijn[1], Sara Gago[1], Takanori Furukawa[1], Alma Morogovsky[5], Ronen Ben Ami[5], Paul Bowyer[1], Nir Osherov[5], Thierry Fontaine[6], Gustavo H. Goldman[2], Emilia Mellado[3], Michael Bromley[1] and Jorge Amich[1,3,*].

1. Manchester Fungal Infection Group (MFIG), Division of Evolution, Infection, and Genomics, Faculty of Biology, Medicine and Health, University of Manchester, United Kingdom.
2. Faculdade de Ciências Farmacêuticas de Ribeirão Preto, Universidade de São Paulo, Ribeirão Preto, Brazil.
3. Mycology Reference Laboratory (Laboratorio de Referencia e Investigación en Micología LRIM), National Centre for Microbiology, Instituto de Salud Carlos III (ISCIII), Majadahonda, 28222 Madrid, Spain.
4. Bioinformatics Core Facility, Faculty of Biology, Medicine and Health, University of Manchester, United Kingdom.
5. Department of Clinical Microbiology and Immunology, Sackler School of Medicine Ramat-Aviv, Tel-Aviv. Sackler Faculty of Medicine, Tel Aviv University, Tel Aviv, Israel.
6. Institut Pasteur, Université de Paris, INRAE, USC2019, Unité Biologie et Pathogénicité Fongiques, F-75015, Paris, France.

# These authors contributed equally. They are ordered alphabetically

* Corresponding author: jamich@isciii.es

ABSTRACT

Aspergillus fumigatus is a filamentous fungus that can infect the lungs of patients with immunosuppression and/or underlying lung diseases. The mortality rates associated with chronic and invasive aspergillosis infections remain very high, despite availability of antifungal treatment. In the last decade, there has been a worrisome emergence and spread of resistance to the azole class of antifungals, which are the first line therapy for the treatment of *A. fumigatus* infections. The mortality caused by resistant isolates is even higher, and the management of these patients is complicated as the therapeutic options are severely reduced. Nevertheless, treatment failure is also common in patients infected with azole susceptible isolates, which can be due to several non-mutually exclusive reasons, such as poor drug absorption. In addition, the phenomena of tolerance or persistence, where susceptible pathogens have the ability to survive the action of an antimicrobial for extended periods of time, have been associated with treatment failure in bacterial infections, and their occurrence in fungal infections already proposed. Here, we investigated the *A. fumigatus* response to the azole voriconazole and demonstrate that certain isolates of this fungal pathogen can display persistence to this antifungal. A sub-population of the persister isolates can survive for extended periods and even grow at a slow rate in the presence of supra-MIC (minimum inhibitory concentration) of voriconazole. Persistence cannot be eradicated with adjuvant drugs or antifungal drug combinations and reduces the efficacy of treatment in a *Galleria mellonella* model of infection. Furthermore, persistence implies a distinct transcriptional profile, demonstrating that it is an active response to the drug. For all these reasons, we propose that azole persistence may be a relevant and underestimated factor that influences the outcome of infection in human aspergillosis.

53 **INTRODUCTION**

54 *Aspergillus fumigatus* is the most prominent fungal pathogen of the human lung, being the major
55 causative agent of a range of diseases collectively termed aspergillosis [1]. The incidence of fatal
56 aspergillosis infections is on the rise due to the increase in the at-risk population [2, 3], including
57 severe COVID-19 patients [4-6]. The mortality associated with *A. fumigatus* infections remains
58 unacceptably high: 38% 5-year mortality rates for chronic pulmonary aspergillosis [7] and ranging
59 from ~35% in early diagnosed and treated patients to nearly 100% if diagnosis is missed or delayed
60 in invasive aspergillosis [8]. These number represent the highest mortality of all invasive fungal
61 diseases [9]. This situation has become even more worrisome due to the emergence of clinical
62 resistance to existing antifungals, which poses a serious threat to human health [10]. Azoles are
63 currently the only FDA-approved class of mould-active agents that can be administrated orally and
64 intravenously, and accordingly they are used for both the evidence-based treatment and prevention
65 of aspergillosis diseases [11]. However, in the last decade, the number of clinical *A. fumigatus*
66 isolates that are resistant to triazole drugs has increased worldwide, causing serious problems for
67 clinical management, as the therapeutic options are reduced and the mortality rates caused by
68 resistant isolates are higher [7, 12, 13]. Furthermore, both in clinical disease and in experimental
69 animal models, it has been observed that treatment failure is common even if the infecting fungal
70 isolate is susceptible to the azole used for treatment [14, 15]. There are several possible
71 explanations for treatment failure in these cases, including antifungal tolerance or persistence [16,
72 17].

73 In the last decade there has been a revolution in our understanding of how pathogenic
74 microorganisms withstand the challenge of antimicrobial drugs. Classically, pathogens were
75 described to be either susceptible or resistant to a certain drug. Antimicrobial resistance is due to a
76 genetic feature in the microbe (intrinsic or acquired *via* mutations) that enables it to grow normally
77 at high concentrations of the agent, above the Minimum Inhibitory Concentration (MIC) defined for
78 the antimicrobial based on the clinical breakpoint. However, in recent years it has become obvious
79 that microbes can withstand the action of drugs by at least three other mechanisms: tolerance,
80 persistence, or heteroresistance. These three phenomena share the feature that they are not
81 triggered by mutations in the microbe's DNA sequence, yet differ in other details. Drug tolerance has
82 been defined as the ability of all cells of a genetically isogenic strain to survive, and even grow at
83 slow rates, for extended periods in the presence of drug concentrations that are greater than the
84 minimal inhibitory concentration (MIC). In persistence, only a small fraction of the isogenic
85 population (usually <1% of the cells) survive, and grow at slow rates, for an extended period of time
86 in the presence of supra-MIC concentrations of the drug [18, 19]. These two phenomena do not

87 imply an increase in the MIC. Finally, heteroresistance is the transient capacity of a microbial
88 subpopulation to increase the MIC in the presence of the drug, due to adaptation, epigenetic
89 modifications or reversible aneuploidy. All those phenomena have been implicated in treatment
90 failure and relapse in bacterial infections [18, 20].

91 In fungi, tolerance has been often described as "trailing growth" and its relevance for infection has
92 been mostly disregarded. However, a recent landmark study in *Candida albicans* has characterised
93 tolerance as a distinct, strain-specific feature and provided evidence for its relevance in persistent
94 candidemia [17, 21]. In *Aspergillus*, trailing growth is known to be prominent in the presence of
95 caspofungin [22, 23] apparently due to single strain heterogeneity [24]. Moreover, at higher
96 concentrations of this drug some isolates can resume normal growth, an effect known as "Eagle" or
97 paradoxical effect (see review [25] for more information), which we have recently demonstrated as
98 a tolerance phenotype [26]. The possible relevance of the paradoxical effect in clinical practice is still
99 under debate, but there is evidence suggesting that it might be important [27], and concern has
100 been raised by some clinicians [28]. Remarkably, it seems that the phenomenon of tolerance in fungi
101 is seen with static drugs, e.g. azoles for *C. albicans* and echinocandins for *A. fumigatus*. However, the
102 possibility that *A. fumigatus* can display tolerance or persistence to azole antifungals had not been
103 previously investigated. Interestingly, in contrast to *C. albicans* and *Cryptococcus neoformans*, azoles
104 have been shown to have fungicidal activity against *A. fumigatus* [29-31], which implies that the
105 underlying mechanisms are likely different. Whilst these phenomena have so far only been
106 investigated in bacteria or yeasts, the approaches to detect and investigate azole tolerance or
107 persistence need to be tailored in filamentous fungi, like *A. fumigatus*, as these organisms form
108 multicellular hyphae. Using various complementary approaches, here we show that small
109 subpopulations of certain *A. fumigatus* isolates can survive and even grow at slow rates at supra-MIC
110 concentrations of the fungicidal drug voriconazole.

111

112 **RESULTS**

113 **Some *Aspergillus fumigatus* isolates show persistence to voriconazole**

114 To determine whether *A. fumigatus* can display tolerance or persistence to voriconazole, we
115 examined a collection of isolates consisting of 9 environmental, 10 clinical (gift from Prof Paul Dyer,
116 collection PD-47-XX, here shortened as PD-XX), 5 common laboratory strains and one resistant
117 control (RC) harbouring the TR34/L98H mutations in the *cyp51A* locus (Table S1) using disc diffusion
118 assays. We evenly spread 4×10^4 conidia of the isolates on RPMI agar plates, placed a 6 mm disc in
119 the centre, containing 10 µL of voriconazole (0.8 mg/mL), and incubated them for 5 days. We

120 observed variability in the sizes of the inhibition halos, reflecting differences in susceptibility of the
121 isolates (Figs. 1A and S1). As expected, the RC strain did not show a proper inhibition halo (Figs. 1A
122 and S1). In contrast, 15 of the 20 isolates showed a clear and well-defined inhibition zone.
123 Interestingly, we found that 5 isolates were able to form colonies within the halo of inhibition, and 4
124 in 5 of these isolates (PD-9, PD-104, PD-254 and PD-266, Fig. S1) formed only a few small colonies,
125 which might be indicative that a few conidia are able to germinate and grow at a slow rate in the
126 presence of a supra-MIC concentration of voriconazole (Fig. 1A and S1). The remaining isolate (PD-
127 256) did not show any inhibition halo, suggesting that it is a resistant isolate.

128 We then assessed the MICs of the original isolates and their derived colonies of the halo (CoHs). A
129 complication of working with a filamentous fungus is that the CoHs need to be grown on a new plate
130 in order to harvest spores (conidia) to be used for MIC determination. We therefore decided to
131 assay two different conidia-harvesting conditions to distinguish the different phenotypes: re-growing
132 the CoHs on solid RPMI in the absence or in the presence of a low concentration of voriconazole
133 (0.12 µg/mL). It would be expected that for conidia grown in the presence of the drug, both
134 resistance and heteroresistance are detected as an increment in the isolate's MIC. In contrast, for
135 conidia grown in the absence of the drug, the reversible increase in MIC that is characteristic of
136 heteroresistance would be lost, whilst a stable genetic-based increment in MIC that defines
137 resistance would be maintained. Finally, persistence should not cause a change of the isolate's MIC
138 independently of the presence of the drug in the conidia-harvesting medium. Using conidia obtained
139 from both conditions, absence and presence of voriconazole, we found that the original isolate did
140 not show an inhibition halo (PD-256, Fig. 1A and S1) had a very high MIC (>8 µg/mL), demonstrating
141 that it is a resistant isolate (Table 1). CoHs formed by PD-254 and PD-266, which upon re-inoculation
142 did not show an inhibition halo (Fig. S1), showed an increased MIC compared to the parental isolate
143 (Table 1). The colony picked from PD-254 showed increased MIC when re-grown on both media with
144 and without voriconazole, suggesting that the CoH may have acquired a mutation that confers a
145 stable resistance phenotype. In contrast, PD-266, which already had an elevated MIC, only showed
146 an increased MIC when re-grown on medium containing voriconazole, suggesting that this strain
147 may be heteroresistant. Finally, CoHs from isolates PD-9 and PD-104 showed the same MICs as their
148 original isolates after a passage in the absence or presence of voriconazole (Table 1). This suggests
149 that they are not resistant or heteroresistant derivatives of the original isolates. Indeed, repetition of
150 the disc assay with the original isolates and with CoH re-grown in the presence of voriconazole,
151 showed a similar level of colony appearance in the original strains and their derived CoHs for PD-9
152 and PD-104 (whereas it grew to the edge of the disc for PD-266, reflecting again a transient increase
153 in its MIC) (Fig. S1). Interestingly, all isolates showed a small increase (one dilution) in MIC when re-

154 grown in the presence of drug (Table 1). This may be due to the development of conidia adapted to
155 the growing environment in preparation for the subsequent germination, an effect recently
156 described in *Aspergillus spp* [32]. To verify that the persistence phenotype is stable, we sequentially
157 passaged CoHs isolated from PD-9 and PD-104 on PDA media (without voriconazole) and performed
158 disc diffusion assays every two passages. The halo of the disc and the relative level of persistence
159 were maintained for as long as we reached (7 passages, Fig. S2), demonstrating that persistence is a
160 stable phenotype.

	Voriconazole MIC (µg/mL)				
Isolate	**original**	**Original (grown on Drug)**	**CoH (- Drug)**	**CoH (grown on Drug)**	**Classification of CoH**
ATCC	1	2			Susceptible
PD-9	0.5	1	0.5	1	Persister
PD-104	1	2	1	2	Persister
PD-254	2	2	>8	>8	Resistant
PD-256	>8	>8	>8	>8	Resistant
PD-266	4	8	4	>8	Heteroresistant

161 **Table 1**. Voriconazole MICs of original isolates and their derived CoHs, pre-grown both in the
162 absence and presence of a low (0.12 µg/mL) concentration of voriconazole

163

164 In bacteria, persister and tolerant cells are often dormant and do not grow [19]. To investigate this in
165 *A. fumigatus* in more detail, we followed a protocol to detect tolerance/persistence in bacteria in
166 which the disc containing the drug, after a period of incubation, is switched, with another one
167 containing fresh media [33]. The rationale is to detect surviving cells that have remained dormant
168 and resume growth after the drug is withdrawn. After initial growth we substituted the disc with
169 voriconazole for a new one containing *Aspergillus* Minimal Media (AMM). Interestingly, after the
170 disc switch colonies were observed in the halos for several isolates (PD-7, -8, -50, -154, -249, and -
171 264, Fig. S3), suggesting that these may be low level persister isolates. Nevertheless, three isolates,
172 PD-9, -104 and -259, were able to form colonies before the disc switch, and of these three, only PD-9
173 and PD-104 grew even more colonies after disc switch (Fig. S3). Therefore, the isolates PD-9 and PD-
174 104 were able to survive and grow at slower rates in the presence of supra-MIC concentrations of
175 voriconazole, a phenomenon that complies with the definition of persistence.

176 To further characterize persistence in *A. fumigatus*, we performed MIC assays with selected strains
177 and checked microscopic growth of persister and non-persister isolates at supra-MIC concentrations.
178 We found that 72 hours after inoculation the non-persister strains ATCC46645 and PD-60 displayed
179 microscopic growth only at the MIC concentration, and no growth at all at higher concentrations
180 (Figs. 1B and S3). In contrast, the persister isolates PD-9 and -104 showed noticeable microscopic

181 growth at 2X, and even at 3X MIC germinated conidia could be detected (Fig. 1B and S3). While the
182 level of growth was variable among independent experiments, the difference between persister and
183 non-persister isolates was consistently observed (Fig. 1B and S4). In addition, we plated the entire
184 content of the wells containing the highest concentrations of voriconazole (8 µg/mL) and found that
185 48 h after inoculation the non-persister strains were nearly all killed (only ~0.07% of the conidia
186 survived) whilst in the persister strains a significantly higher ratio of conidia survived (0.39% of PD-9
187 p=0.002 and 0.18% of PD-104 p=0.0331, Fig. 1C). Therefore, a subpopulation of the *A. fumigatus*
188 persister isolates can survive for long periods in the presence of high concentrations of voriconazole
189 and even grow at a slow rate, which seem to be inversely correlated with the concentration of drug.

190 In bacteria, a combination of MIC and speed of killing is the best approach to reveal and differentiate
191 tolerance and persistence [18]. Therefore, we investigated the dynamics of cell death caused by
192 voriconazole for persister and non-persister isolates. Conidia from two susceptible (ATCC46645 and
193 PD-60), two persister (PD-9 and PD-104) and the putative heteroresistant (PD-266) strains were
194 incubated for 4 days in liquid RPMI in the presence of 4 µg/mL of voriconazole and aliquots of the
195 culture plated (after PBS washing to remove the drug) on PDA rich media every 24 hours (Fig. 1D).
196 We found that for all strains the number of viable conidia dramatically declined after 24 hours of
197 incubation, reflecting a strong fungicidal action of voriconazole, even against an isolate with high
198 MIC. Interestingly, whilst the susceptible isolates were completely killed within 48-72 hours, a
199 considerable number of conidia from the persister strains maintained viability for an extended
200 period of time (~0.748% for PD-9, ~0.136% for PD-9 at 48 h and ~0.52% for PD-9, ~0.128% for PD-9
201 at 72 h, Fig. 1D), resulting in the characteristic biphasic killing curve that is the hallmark of
202 persistence [19]. The isolate PD-266 showed visible growth from 72h, which agrees with its proposed
203 heteroresistant phenotype, and saturated the plate at the last time-point. To investigate the survival
204 of the isolates at the single cell (conidial) level, we incubated the two persister and one susceptible
205 strains in liquid RPMI in the presence of 32 µg/mL voriconazole for 48 hours, and replaced it with
206 fresh drug free medium. We observed that during the first 24 hours of incubation after drug
207 withdrawal there was no growth for any of the isolates, but subsequently the persister strains were
208 able to resume growth (Videos S1 and S2) whilst the susceptible strain was not (Video S3). Hence,
209 persister strains indeed can survive for extended periods in the presence of high concentrations of
210 voriconazole and resume growth when the drug is withdrawn.

211 To check if the observed phenomena could be explained by mutations in the azole target genes, we
212 sequenced the promoter and ORF of *cyp51A* and the ORF of *cyp51B* in the persister isolates PD-9
213 and PD-104 and the non-persister strain PD-60. In all strains we found that *cyp51A* was completely
214 wild-type (there were no nucleotide changes) and *cyp51B* had only synonymous polymorphisms

215 (Table S2), thus denying an implication of target enzyme mutations in the phenomenon of
216 persistence. We also sequenced the sterol-sensing domain of *hmg1*, as it has been proposed that
217 mutations in this gene may be a precursor step for the development of azole resistance [34, 35], and
218 in bacteria persistence has been shown to correlate with the evolution of resistance [36, 37].
219 However, we found again that all strains harboured a completely wild-type sequence (not shown),
220 suggesting that *hmg1* is not related with voriconazole persistence.

221 In conclusion, we have observed that certain *A. fumigatus* isolates can survive and grow at slow
222 rates for extended periods of time in the presence of supra-MIC concentrations of voriconazole,
223 therefore, these isolates display persistence to voriconazole.

224 ***Aspergillus fumigatus* persistence is maintained in the hyphal transition and seems to be medium**
225 **dependent.**

226 *A. fumigatus* undergoes morphological changes during its development, shifting from resting conidia
227 to swollen conidia (~4-5 h), then to germlings (~8 h) and finally forming hyphae (~16 h). As the
228 cellular metabolic status is different at each developmental stage [38], we speculated that it might
229 influence the capacity of the fungus to deploy persistence in the presence of voriconazole. To
230 investigate this possibility, we incubated the RPMI plates inoculated with the fungus for 8 or 16
231 hours before adding the drug to the disc. We found that the persister strains PD-9 and PD-104 were
232 also able to form colonies in the halo when drug was added 8 hours after the beginning of
233 incubation (Fig. 2A), suggesting that persistence is not determined by the developmental stage. We
234 could not draw definitive conclusions for the 16 hours grown hyphae, as the background growth was
235 too dense to undoubtedly differentiate specific persister colonies (Fig. 2A). Nevertheless, we could
236 clearly detect a growing colony in the voriconazole halo for the strain PD-104 (Fig. 2A), proving that
237 at least this strain can display persister growth when short hyphae are challenged with the drug.
238 Interestingly, it has previously been reported that morphological status alters *A. fumigatus*
239 susceptibility profiles against various drugs including voriconazole [39], which supports the notion
240 that persistence is a different phenomenon, triggered by distinct mechanisms, and independent of
241 MIC.

242 To determine if persistence is influenced by the growth medium, we performed a voriconazole disc
243 diffusion assay with the PD-104 isolate and the wild-type control ATCC46645 on PDA rich media or
244 AMM. The PD-104 strain showed persister growth on both media, and it seemed to be able to form
245 a higher number of COHs on PDA rich media (Fig. 2B). The ATCC46645 wild-type strain did not show
246 persistence on AMM, but surprisingly it did form colonies in the halo on PDA media (Fig. 2B). To
247 investigate this in more detail we repeated the disc assay using two different rich media, PDA and

248 Sabouraud, with more strains, CEA10, PD-9, and PD-60 (Fig. 2C) and found that all strains were able
249 to form colonies in the halos. The MICs of the isolates, measured by broth dilution assay, were equal
250 on Sabouraud and RPMI (Fig. 2D), indicating that the effect of the drug is not reduced in rich
251 medium. Therefore, the ability of *A. fumigatus* to display persistence seems to be medium
252 dependent, suggesting that a rich nutrient environment favours survival at supra-MIC
253 concentrations. This is supported by a recent study that showed that a rich metabolic environment
254 can promote azole tolerance in *Saccharomyces cerevisiae* [40]. Nevertheless, it should also be
255 considered that voriconazole diffusion may be affected in solid rich media, which could be
256 confounding this observation.

257 ***Aspergillus fumigatus* persistence to voriconazole is independent of stress and cannot be inhibited**
258 **with adjuvant or antifungal drugs.**

259 Changing environmental conditions activate signalling cascades that trigger transcriptional
260 adaptation and cell wall alterations [41-44]. Therefore, we reasoned that the capacity of certain
261 isolates to survive and grow in supra-MIC concentrations of voriconazole might be influenced by
262 environmental stressors. Indeed, in *C. albicans* mutants and inhibitors of stress response pathways
263 eliminate tolerance [45]. To investigate this possibility, we analysed voriconazole persistence of PD-
264 104 in the presence of hypoxic (1% O_2), oxidative (0.01% H_2O_2), osmotic (150 mM NaCl), membrane
265 (0.05% SDS) and cell wall (10 µg/mL CalcoFluor White) stress. Surprisingly, in contrast to *C. albicans*
266 [21], we found that most environmental conditions did not influence persistence in *A. fumigatus*
267 (Fig. 3A). This suggests that the underlying mechanism(s) of persistence in *A. fumigatus* are likely
268 different from the previously proposed mechanisms of tolerance in *C. albicans*. The only condition
269 that influenced *A. fumigatus* persistence was hypoxia, which could prevent growth in the halo (Fig.
270 3A). As we had observed above that persistence was influenced by the growth medium, we
271 wondered if hypoxia could prevent persistence also on rich medium. As shown in Figs. 2B and 2C, all
272 isolates were able to grow colonies in the halo when grown on the rich medium YAG on normoxia
273 (Fig. 3B). However, persistence was eliminated under hypoxia for all strains, except for PD-104, for
274 which it was reduced but apparently not completely eradicated. Therefore, it seems that hypoxia
275 reduces persistence, but the nutritional composition of the medium also influences its impact on the
276 phenomenon.

277 In *C. albicans*, fluconazole tolerance (but not resistance) can be prevented with the use of adjuvant
278 drugs that block general stress signalling pathways [21]. To further investigate if the underlying
279 mechanism of persistence may be different in *A. fumigatus*, we tested the effect of various drug
280 adjuvants that were previously shown to eliminate tolerance in *C. albicans* [21]: geldanamycin (0.8
281 µg/mL), an inhibitor of heat shock protein (Hsp90) [46, 47], FK506 (4 ng/mL), an inhibitor of

282 calcineurin [48], H-89 (4 µg/mL), an inhibitor of the cAMP-dependent protein kinase (PKA) [49],
283 rapamycin (6.25 µg/mL), an inhibitor of the mammalian target of rapamycin (mTOR) [50], and
284 tunicamycin (10 µg/mL), an inducer of the unfolded protein response pathway [51]. In contrast to *C.*
285 *albicans*, the use of adjuvant drugs did not prevent persistence of *A. fumigatus* isolates (Fig. 3C). We
286 also tested lovastatin (8 µg/mL) and simvastatin (2 µg/mL), as statins inhibit 3-hydroxy-3-
287 methylglutaryl-coenzyme A (HmgA) [52], an enzyme in the same metabolic pathway as the target of
288 azoles, and these two were previously shown to have antifungal activity against *Aspergillus spp* [53].
289 However, statins were also not able to prevent persister growth (Fig. 3B). Finally, as efflux of
290 antifungals has been proposed to play a role in *C. albicans* tolerance [45], we tested if the efflux
291 inhibitors milbemycin A oxim (8 µg/mL) [54] or clorgyline (63.5 µg/mL) [55] can prevent *A. fumigatus*
292 persistence. These compounds seemed to be able to diminish the persister capacity of the strains, as
293 only one CoH per plate could be detected, and these colonies were exactly at the edge of the halo
294 (Fig. 3C). In conclusion, adjuvant drugs cannot prevent *A. fumigatus* persistence to voriconazole, and
295 efflux inhibitors may affect this process and deserve further study.

296 Next, we evaluated if persistence can be eradicated using combinatorial treatment with the other
297 classes of antifungal drugs in clinical use. However, neither amphotericin-B (1 µg/mL) nor
298 caspofungin (0.5 µg/mL) could prevent persistence (Fig. 3D). Interestingly, these antifungal drugs
299 could also not impede growth in the halo of the presumed heteroresistant strain PD-266 (Fig. 3D).
300 Therefore, it seems that combinatorial treatment with other antifungals cannot prevent persistence
301 in *A. fumigatus*.

302 **The phenomenon of persistence can be observed with other azole drugs**.

303 To check if *A. fumigatus* can display persistence in the presence of other azoles, we firstly employed
304 the disc diffusion assay adding 10 µL of a 3.2 mg/mL itraconazole solution. We found that the
305 isolates PD-104 and PD-266 were able to form colonies in the halo (Fig. S5). Upon re-inoculation of a
306 CoH (re-grown in itraconazole containing media), the isolate PD-104 showed an inhibition halo of the
307 same size and displayed similar level of CoH appearance, whereas the PD-266 isolate was able to
308 grow on the whole plate and did not show any inhibition halo. Therefore, this suggests that, as
309 observed with voriconazole, the isolate PD-104 is persistent and the isolate PD-266 is
310 heteroresistant to itraconazole. We then performed a broth dilution assay with our four well-
311 characterised isolates (non-persisters ATCC46645 and PD-60 and persisters PD-9 and PD-104) to
312 calculate the MIC for itraconazole and isavuconazole, and looked under the microscope at supra-MIC
313 concentrations (Fig. S6A and S6B). We found that the isolates PD-9 and PD-104 showed slight growth
314 at 2X MIC, whilst ATCC46645 and PD-60 did not (Fig. S6B). Moreover, we inoculated the entire
315 content of wells containing the highest concentration of the drugs (8 µg/mL) on PDA plates, and

316 found that a detectable number of conidia from the isolates PD-9 and PD-104 remained viable after
317 48 hours of incubation in the presence of the azoles (Fig. S6C). Hence, even if more experiments
318 need to be done for a detailed characterization of persistence to these azoles, these results suggest
319 that the same isolates that are persisters to voriconazole could also display persistence to
320 itraconazole and isavuconazole.

321 **The transcriptome of persister growth suggest that Galactosaminogalactan and high expression of**
322 **sterol biosynthetic genes may be relevant to establish persistence.**

323 To better understand the heterogeneous nature of persistence, we compared the transcriptome of
324 PD-104 grown under conditions favouring persistence (above MIC), sub-MIC and in the absence of
325 drug. We inoculated the spores on top of a nylon membrane placed on an RPMI solid plate. We put
326 the disc with voriconazole (0.8 mg/mL) on the membrane and incubated for 5 days at 37°C. Standard
327 halos of inhibition formed on the membrane, and persister colonies appeared for the PD-104 strain,
328 but not for the A1160 strain (Fig. S7A). We harvested mycelium (avoiding conidia as much as
329 possible) from plates without a voriconazole disc (No Drug), from the area equidistant from the
330 border of the plate and the inhibition halo (Low Drug) and the colonies in the halo (Persistence) (Fig.
331 4A). We had to combine persister colonies from 20 plates per replicate in order to obtain sufficient
332 material for RNA extraction. Additionally, we harvested mycelia from A1160 with No and Low Drug
333 under the same conditions. We performed RNA-seq and compared the transcriptomes of the
334 following conditions (i) A1160 Low Drug VS No Drug, (ii) PD-104 Low Drug VS No Drug, (iii) PD-104
335 Persistence VS No drug and (iv) PD-104 Persistence VS Low Drug. We considered as differentially
336 expressed genes (DEG) those with a log2FoldChange >1 or <-1 and a false discovery rate (FDR) <0.05.

337 In A1160, we detected 62 genes significantly upregulated in the presence of low voriconazole
338 concentrations and only 4 that were downregulated (Fig. 4A and Dataset S1). Such a low number of
339 DEGs may be due to the relatively low concentration of voriconazole in the harvested area.
340 Nevertheless, among the upregulated genes we found 10 related to sterol biosynthesis (Dataset S1),
341 including *cyp51A* and *cyp51B*, the expression of which have been reported to increase upon azole
342 challenge [56, 57]. Surprisingly, only 21 of the 62 upregulated genes overlapped with our previously
343 published dataset, in which 1492 genes were upregulated upon challenge of A1160 with itraconazole
344 [58]. This striking difference may be due to the different drug employed, the different
345 concentrations assayed and/or the use of solid medium. Interestingly, these 41 DEGs that are
346 specific to this analysis (which can be found in Dataset S1) contain *cyp51A*, *cyp51B* and various other
347 genes of the sterol pathway.

348 For PD-104, the Low Drug VS No Drug comparison retrieved 32 genes upregulated and only 1
349 downregulated (Fig. 5 and Dataset S2). Within the upregulated genes we again found 8 genes
350 related with sterol biosynthesis, including *cyp51A*. In addition, 9 genes did not overlap with the
351 comparison of A1160 (Fig. 4A and Dataset S2). These differences with A1160 may point to potential
352 strain differences in response to voriconazole. In the Persister VS No Drug comparison there were
353 802 upregulated and 249 downregulated genes and in the Persister VS Low Drug 646 upregulated
354 and 187 downregulated genes (Fig. 4A and Dataset S2). When comparing those three analyses, only
355 53 genes were exclusively upregulated and 39 downregulated in Persister VS Low Drug (detected
356 using BioVenn [59]), suggesting that they may be important to establish the persister phenotype and
357 not only as a response to the drug (Fig. 4A and Dataset S2). We performed Gene Ontology (GO)
358 enrichment analyses (on FungiDataBase [60]) for these 53 DEGs, which retrieved a number of
359 biological processes and molecular functions for up- and downregulated genes. It is important to
360 note that the FDR did not reach significance for any of them, which is possibly due to the low
361 number of genes included in the analysis. However, we believe this analysis provided interesting
362 clues and can help to direct future research. For the up-regulated genes, the strongest enrichment
363 was for the biological processes galactose and aldehyde metabolisms (Fig. 4B) and the molecular
364 function oxidoreductase activity (Table S3). Interestingly, galactose metabolism was found to be the
365 most upregulated function in *Staphylococcus aureus* persisters, although the reason has not been
366 elucidated yet [61]. For the downregulated genes, there was an enrichment of biological processes
367 related with development and cell cycle (Table S3), possibly reflecting the reduced growth rate in
368 this condition.

369 Interestingly, a significant number of the detected differentially expressed mRNAs in PD-104 were
370 not assigned to any gene of the A1163 genome reference used for the mapping of the reads. In
371 detail, 80 of the upregulated (including 4 of the 20 most upregulated) and 29 of the downregulated
372 for the Persister VS no Drug comparison and 55 upregulated (including 5 of the 10 most
373 upregulated) and 14 downregulated for the Persister VS no Low comparison seem to have no
374 orthologue in A1163 (Dataset S2). This points to the requirement of a high number (~10% of the
375 DEG) of strain specific genes to facilitate for persister growth. Therefore, we re-annealed the
376 sequenced mRNAs from the PD-104 isolate to the newly generated *A. fumigatus* pangenome [62]
377 and performed the comparisons again (Dataset S3). In this analysis, the Persister VS no Drug
378 comparison retrieved 811 genes up- and 260 downregulated, and the Persister VS Low Drug
379 comparison 659 up- and 193 downregulated (Fig. 4A and Dataset S3). The ratio of identified genes
380 greatly improved, as only ≤1.8% of the DEGs could not be assigned to an ID. Yet, the most
381 upregulated gene in the Persister VS Low Drug comparison was an unidentified gene and many of

382 the newly identified genes encode uncharacterised hypothetical proteins, which reflects our
383 ignorance of *A. fumigatus* biology and thus how difficult it is unravelling underlying mechanisms in
384 this pathogen. GO enrichment analysis of all DEGs showed that secondary metabolism, ergosterol
385 metabolism and transport were key upregulated biological processes (Fig. 4C) and oxidoreductase,
386 catalysis and transmembrane transport important molecular functions (Table S4), all of which
387 suggests an active metabolic response in persister conditions. As observed above (Table S3),
388 downregulated biological processes reflected a downregulation of developmental processes (Table
389 S4). Comparison of the DEGs present in all three comparisons revealed that 64 genes were
390 exclusively up- and 46 downregulated in Persister VS Low Drug (detected using BioVenn [59]),
391 suggesting that they may be specifically important for persistence (Fig. 4A and Dataset S3). GO
392 enrichment analysis of those genes revealed galactosaminogalactan (GAG) biosynthesis as the most
393 significant upregulated biological process (Fig. 4D and Table S5), providing a plausible explanation
394 for the upregulation of galactose metabolism observed before, and suggesting that this
395 exopolysaccharide may be relevant for persistence in *A. fumigatus*. Next, we performed a protein
396 functional association analysis using the STRING database and platform [63] to investigate if these 64
397 upregulated genes are functionally correlated. Sixty-one of these genes could be matched to
398 proteins in the database, showing a significant (p=1.84e-08) interaction network, including a node of
399 17 proteins related with metabolism (Fig. S7B and Table S6). This suggests that a distinct metabolic
400 response occurs during persister growth.

401 Bacterial persistence has been proposed to be a sub-population event due to stochastic high
402 expression of relevant genes [64, 65]. Accordingly, we reasoned that those genes that are
403 upregulated in Low Drug VS No Drug and Persister VS No Drug comparisons, but also in Persister VS
404 Low Drug might reveal those genes that are important to adapt to presence of the drug, but also
405 that can create persistence with higher levels of expression. We identified 18 genes that appeared as
406 upregulated in all three comparisons (Fig. 4A and Table 2), indicating that they have higher levels of
407 expression in persistence VS normal response to the drug. GO enrichment analysis revealed sterol
408 metabolism as the most significantly upregulated biological process (Fig. 4E and Table S7). Indeed,
409 those few genes had a very significant enrichment in the KEGG pathway "steroid biosynthesis"
410 (Table 2), suggesting that high expression of genes in the sterol biosynthetic route (including *cyp51A*)
411 may enable the sub-population of persisters to survive and grow in supra-MIC concentrations.
412 Additionally, these highly expressed genes were enriched in KEGG pathways related with
413 cytochrome P450 dependent drug metabolism (Table 2), which may indicate that detoxification of
414 azoles is also important for persistence. Finally, expression of the *cdr1B* transporter
415 (AFUA_1G14330), known to be associated with azole resistance [66], was also detected to be higher

416 in persistence (Table 2). This suggests that a higher capacity to efflux azoles may also be important
417 for the persister phenotype. Finally, we performed a protein functional association analysis with
418 these 18 genes using the STRING database and platform [63] to search for functional correlations. All
419 18 genes were matched to proteins and a significant interaction (p<1.0e-16) was found, involving a
420 highly interactive nodule of 6 proteins related with steroid biosynthesis (Fig. S7C and Table S8),
421 suggesting again that a high production of ergosterol is important for persistence.

422

423

Gene ID	Product description
AFUA_1G03200	Putative major facilitator superfamily (MFS) transporter
AFUA_4G06890	14-alpha sterol demethylase Cyp51A
AFUA_2G00320	putative sterol delta 5,6-desaturase
AFUA_3G00810	Putative cholestenol delta-isomerase
AFUA_1G03150	C-14 sterol reductase, putative
AFUA_8G02440	C-4 methyl sterol oxidase, putative
AFUA_6G14140	Has domain(s) with predicted role in response to stress and integral component of membrane localization
AFUA_3G00150	Has domain(s) with predicted oxidoreductase activity and role in metabolic process
AFUA_4G01440	Predicted glutathione S transferase
AFUA_4G04820	C-4 methyl sterol oxidase Erg25, putative
AFUA_5G00840	Ortholog of *A. nidulans* FGSC A4 : AN5639, AN2587, AN9444, AN7395,
AFUA_2G15130	ABC multidrug transporter A-2, putative
AFUA_5G03290	Ortholog of *A. nidulans* FGSC A4 : AN8197, A
AFUA_3G02520	Has domain(s) with predicted role in transmembrane transport and integral component of membrane localization
AFUA_7G04740	Ortholog of *A. fumigatus* Af293 : Afu1g01960, Afu3g01040, Afu3g03315, Afu7g01960, Afu8g05750, Afu5g00135, Afu7g06526
AFUA_2G01890	Ortholog(s) have 2-octoprenyl-3-methyl-6-methoxy-1,4-benzoquinone hydroxylase activity,
AFUA_1G14330	Azole transporter
AFUA_8G00710	Has domain(s) with predicted role in defense response, negative regulation of growth

KEGG Pathway			
ID	Name	P-value	Benjamini
ec00100__PK__KEGG	Steroid biosynthesis	2,31E-08	1,18E-06
ec00980__PK__KEGG	Metabolism of xenobiotics by cytochrome P450	0.002873	0.07326
c00982__PK__KEGG	Drug metabolism - cytochrome P450	0.004423	0.07520

424 **Table 2**. GO biological processes enrichment and KEGG pathway enrichment for the 18 genes that
425 showed higher expression in Persistence than in NoDrug and LowDrug.

426

427 **Galactosaminogalactan potentiates persistence of PD-104.**

428 Our transcriptome analysis detected a significantly higher expression of two GAG biosynthetic genes
429 (*sph3*, AFUA_3G07900 and *uge3*, AFUA_3G07910) in persister growth (Dataset S3). Manual
430 inspection of the GAG biosynthetic genes [67, 68] revealed that another gene (*agd3*,
431 AFUA_3G07870) might also be upregulated (FC= 1.01), but although the *p*-value was significant (*p*=
432 0.0179), the FDR rate was above threshold (FDR=0.1167) (Dataset S3). This prompted us to
433 investigate if a higher amount of GAG could create and/or potentiate persistence in *A. fumigatus*.
434 To this aim, we performed broth dilution assays in which we inoculated each isolate (ATCC, PD-9,
435 PD-60 and PD-104) in two different lines and added purified GAG at a concentration of 100 µg/mL to
436 one of them. Comparison of the MIC with and without GAG demonstrated that this polysaccharide
437 did not affect the resistance profile of the isolates (Fig. 5A). After reading the MIC at 48 hours, we
438 added 10 µg/mL of the dye calcofluor white (CFW) to the wells and imaged the entire well (87
439 photos using a 20X objective) at the blue emission channel. Images were merged (Fig. 5B) and the
440 number of germinated conidia/short hyphae in the whole well calculated as explained in materials
441 and methods (Fig. 5B). By these means we could calculate that ~2% of the PD-9 spore population
442 and ~1% of the PD-104 conidia were able to germinate at 2X MIC, and ~0.35% for both isolates in 3X
443 MIC. Interestingly, addition of GAG enhanced the number of persisters in PD-104 (from 1.09% to
444 2.80%, *p*=0.0267 at 2X MIC and from 0.41% to 0.75% *p*=0.038) but not in PD-9 (Fig. 5B). Next, we
445 inoculated the four isolates in duplicated lines of 96-well plates containing a high concentration of
446 voriconazole (4 µg/mL) in all wells, and added GAG to one line of each isolate. The entire contents of
447 wells were plated 48 hours after inoculation on PDA rich plates to count the number of viable CFUs.
448 As observed before (Fig. 1C), we found that the persister isolates (PD-9 and PD-104) maintained
449 viability of a significant number of conidia for an extended period of time (Fig. 5C). Interestingly,
450 GAG addition seemed to slightly increase the number of grown CFUs for all isolates, although this
451 increment was only significant for the PD-104 isolate (PD-104 VS PD-104+GAG *p*=0.0437).

452 These results suggest that a high level of GAG can potentiate persistence in some, but apparently
453 not all, isolates. Future investigations will aim to understand the underlying mechanism and to
454 determine why GAG addition is isolate-specific.

455 **Persistence can be detected in diverse *A. fumigatus* collections of isolates**

456 To corroborate that certain *A. fumigatus* isolates display persistence to voriconazole, we decided to
457 screen two independent collection of isolates. Initially, we tested an environmental library of isolates
458 collected in the area of Manchester, UK [69]. We screened all 157 isolates for growth under the

459 microscope after 72 hours incubation in the presence of a high concentration of voriconazole (8
460 µg/mL). We found that 34 isolates were able to show a limited degree of growth, suggesting that
461 they might be persisters (Table S9). Next, we employed disc diffusion assays with 0.8 mg/mL
462 voriconazole and observed that 15 out of the 34 isolates were able to form colonies in the halo
463 (Table S9). Broth dilution assay with the original isolates and the CoHs revealed that 10 of those
464 isolates did not have increased MICs, indicating that they were persister strains (Table S9).
465 Therefore, at least ~6% of this collection was persister to voriconazole. We further evaluated a
466 collection of 17 azole-susceptible clinical isolates obtained from TAU medical centre (Table S9),
467 which were prior shown not to have any mutation in the *cyp51A* gene promoter or ORF, using the
468 disc diffusion assay. We found that 6 out of 17 (35%) isolates were able to grow small colonies in the
469 inhibition halo (Fig. S8A). Colonies picked from within the halo formed upon re-inoculation similar
470 size halos, indicating that the MIC had not increased, and grew a similar number of CoHs, suggesting
471 that the isolates are persisters.

472 Therefore, evaluation of independent collection of isolates seem to always retrieve a significant
473 number of persister strains, demonstrating that this is quite a common phenomenon.

474 **Persistence is not a lineage specific trait.**

475 Recent studies suggest that the tandem repeats (TRs) in the promoter region of *cyp51A*, which cause
476 high levels of antifungal resistance, possibly have evolved in the environment, due to the use of
477 demethylase inhibitors (azoles) in the fields [70]. Interestingly, the isolates with the TR_{34}/L98H
478 polymorphism have been found to be closely related [62, 70], which suggest that this mechanisms
479 has evolved in a distinct lineage of the species. To investigate if the phenomenon of persistence
480 could also be lineage specific, we sequenced the genome of 23 of our isolates, 12 persisters and 11
481 non-persisters (Table S9) and integrated their genome into a recently published phylogenetic
482 analysis [62]. We found that both persister and non-persister isolates scattered through the entire
483 tree, demonstrating that persistence is not a trait of a specific lineage of *A. fumigatus* (Fig. 6). In
484 addition, it is noteworthy that some persister and non-persister isolates seem to be genetically very
485 similar, as they are close in the tree (JA12-JA14-JA7-JA8 and also JA1-JA2, Fig. 6). This suggests that
486 the genetic features that enable persistence are modest and/or that non-genomic features, as the
487 transcriptional response, are important for isolate specificity.

488 **Persister isolates are less efficiently eliminated with a voriconazole treatment in a *Galleria***
489 ***mellonella* infection model.**

490 To evaluate if persistence may be relevant during antifungal treatment, we employed the *Galleria*
491 *mellonella* mini-host model of infection. This model has been successfully used to investigate the

492 efficiency of azole treatment against *A. fumigatus* [71, 72]. In addition, a recent study has
493 characterised the pharmacokinetics of voriconazole in infected larvae, which helped us select the
494 optimal dose to reach a high concentration of the drug in the haemolymph, but that is nearly
495 completely removed in 24 hours [73].

496 Initially, we performed a survival experiment with all four strains to investigate if they could have
497 different virulence potential. We infected larvae with 10^4 conidia of non-persister (ATCC46645 or
498 PD-60) or persister (PD-9 or PD-104) isolates and followed mortality for 10 days. All the isolates
499 killed larvae at a similar rate (Fig. 7A), demonstrating that they are similarly virulent. Therefore, we
500 aimed to use this model to investigate if persistence could potentially cause treatment failure. We
501 reasoned that a voriconazole treatment should very efficiently eradicate susceptible, non-persister
502 strains, but it may not be able to eliminate persister strains with the same efficiency. We infected
503 larvae with 10^4 conidia of non-persister (ATCC46645 or PD-60) or persister (PD-9 or PD-104) isolates,
504 administered one dose of 8 µg/larva voriconazole or PBS at the time of infection, and measured
505 fungal burden 72 hours after infection. As expected, voriconazole treatment was efficient and
506 dramatically decreased fungal burden for all isolates (Fig. 7B). Interestingly, the mean reduction in
507 burden was bigger for non-persisters isolates (55.0X for ATCC46445 and 47.5X for PD-60, Fig. 6B)
508 than for the persisters (9.8X for PD-9 and 15.8X for PD-104, Fig. 6B). Indeed, whilst some larvae from
509 all groups had been completely cured with the treatment, three larvae from both PD-9 and PD-104
510 infected groups still had a considerable fungal burden, whilst only one larva from ATCC46645 or PD-
511 60 had similar levels (Fig. 7B). Therefore, these results suggest that persister strains are less
512 efficiently eliminated by a voriconazole treatment than non-persister isolates *in vivo*.

513

514 **DISCUSSION**

515 The phenomenon of persistence to antimicrobials was first observed in bacteria 80 years ago [74,
516 75]. In the last decade, intensive research has permitted unravelling various underlying mechanisms
517 in diverse bacteria, and it has become clear that persistence can cause treatment failure and lead to
518 the development of resistance [76, 77]. However, our insight into antifungal persistence and
519 tolerance in fungal pathogens is still in its infancy.

520 We have recently shown that all conidia in a tolerant *A. fumigatus* isolate are able to grow at high
521 concentrations of caspofungin [26]. In *C. albicans*, tolerance to fluconazole was described to be a
522 sub-population effect, but the ratio of tolerant cells was reported to be elevated [21]. In both cases,
523 tolerance was observed in response to static drugs, so it seems that the phenomenon of tolerance in
524 fungi associates with fungistatic drugs. In *C. albicans*, the formation of amphotericin-B (AmB)

525 persister cells has been described [78]. Of note, this phenomenon has only been described within
526 biofilms, and cannot be found in planktonic cells [79], possibly due to the physical protection
527 conferred by the biofilm, which may be relevant for the capacity of these cells to survive in the
528 presence of AmB. Indeed, in *A. fumigatus* it was shown that the hypoxic microenvironment
529 developed in biofilms led to reduced metabolic activity in the basal biofilm level leading to the
530 formation of cells that can survive the antifungal challenge, and serve as a drug-resistant reservoir
531 [80].

532 We have observed that a small sub-population (0.1 to 5%) of certain *A. fumigatus* isolates can
533 survive for extended periods and even grow at slow rates in the presence of supra-MIC
534 concentrations of the fungicidal drug voriconazole. In bacteria, tolerance and persistence have been
535 classically explained by a downregulation of metabolism and cell cycle, which trigger a status of
536 dormancy that permit survival despite the action of the drug. However, recent research in
537 pathogenic bacteria has demonstrated that active metabolic responses are required for persistence
538 [81, 82], and slow-growing persisters have also been detected *in vitro* [83] and *in vivo* [84]. Active
539 metabolism may even be advantageous, as in the case of *Salmonella*, where persisters have been
540 shown to undermine host defences [85]. Interestingly, *C. albicans* AmB persistence has been
541 described to involve downregulation of primary metabolism, but also an increase of stress responses
542 and oxidative defensive mechanisms [86]. We have observed that active growth is possible at two or
543 even three-fold the MIC, and that this growth entails a distinct transcriptional profile. Therefore, this
544 phenomenon is not merely survival of dormant conidia in the presence of the drug, but seems to be
545 an active mechanism that enables a sub-population of certain isolates to withstand the action of
546 voriconazole for an extended period. Indeed, using resazurin (an oxidation-reduction indicator used
547 for the measurement of metabolic activity and proliferation of living cells, which use has been
548 optimised for *A. fumigatus* [87]) we could detect a slight metabolic activity at supra-MIC
549 concentrations (Fig. S8B). This might explain why hypoxia is the only environmental condition that
550 reduced persistence, as in low oxygen the metabolic activity is reduced [80] and the energy
551 generating metabolism changes [88].

552 We have observed a big difference in growth between liquid media (only microscopic growth) and
553 solid media (macroscopic colonies). We hypothesise that this may be because in agar drug
554 microdepletions around the hyphae would diffuse back much slower than in liquid, giving an
555 advantage to the hyphae in solid media. In addition, there may be a different level of contact of
556 conidia with the drug; in liquid, the conidia are completely surrounded, whilst on solid media the
557 conidia just lay on the drug and may escape from it by orientating the germling polarity as they
558 grow.

559 The concept of persistence entails two intriguing aspects. Firstly, it is an isolate-dependent
560 phenomenon, which means that there must be a genetic basis that underlies persistence. We have
561 shown that the persister isolates do not belong to a specific lineage, suggesting that this feature has
562 not appeared as an evolutionary trait in a lineage of isolates. Recently, it has been described that
563 each *A. fumigatus* strain carries a particular set of accessory genes, which associates with different
564 levels of virulence and drug resistance capacities [89]. In the same vein, we speculate that the
565 presence or absence of certain accessory genes may enable certain isolates to persist in the
566 presence of azoles. Future research will evaluate if this hypothesis is true. A second intriguing aspect
567 of persistence is that it is a sub-population phenomenon, meaning that within an isogenic isolate
568 only a few conidia are able to survive and grow in the presence of the drug. In bacteria, stochastic
569 expression of key genes has often been proposed as an important underlying cause of persistence
570 [64, 65, 90, 91]. This includes stochastic high expression of genes that directly confer resistance [92]
571 and efflux activity [93]. Similarly, in our RNA-seq analysis we have detected a higher level of
572 expression of genes of the sterol biosynthesis pathway, including *cyp51A*, and of the azole exporter
573 Cdr1B in persister cells. Therefore, it is plausible that stochastic high levels of these genes could
574 generate the capacity to survive for an extended period in the presence of supra-MIC concentrations
575 of voriconazole. Additionally, we detected a higher level of expression of GAG biosynthetic genes,
576 and we have observed that externally added GAG can increase the number of persisters in the
577 isolate PD-104. Interestingly, this polysaccharide did not increase the isolate's MIC, indicating that it
578 does not provide a physical barrier that shields the fungus or that it cannot somehow degrade the
579 drug. Future investigations will aim to unravel why GAG potentiates persistence in PD-104, and not
580 in PD-9, which is interesting as it suggests that there might be multiple persistence mechanisms.
581 GAG is a very relevant *A. fumigatus* virulence factor, with multiple described adhesion and
582 immunosuppressive activities [94, 95], and here we propose that it may have one more important
583 role in potentiating persistence to voriconazole.

584 In bacterial infections, there is significant evidence supporting a role for the phenomena of tolerance
585 and persistence in antibiotic treatment failure [16, 96]. In contrast, the knowledge about these
586 phenomena in fungal infections is still very scarce. Probably, the best-studied phenomenon is
587 heteroresistance in *Cryptococcus neoformans* and *C. gatii* [97-99], which has been found to be a
588 major cause of treatment failure in cryptococcal meningitis [100-104]. As mentioned above, there is
589 already evidence indicating that fluconazole tolerance can cause treatment failure in invasive
590 candidiasis [17, 21], and limited evidence suggests that caspofungin tolerance may cause treatment
591 failure in *Aspergillus* infections [27]. Here, we show that voriconazole treatment seems to eliminate
592 persister isolates less efficiently than non-persister isolates in a *Galleria* model of infection.

593 Therefore, this is the very first evidence to suggest that persistence may reduce the efficacy of
594 voriconazole treatment in *A. fumigatus* infections, which would support the hypothesis that
595 persistence might cause therapeutic failure. In addition to such a potential direct effect of
596 persistence on treatment failure, resilience and relapse of persistent strains could associate with the
597 development of antifungal resistance (an effect that has already been shown for bacterial infections,
598 see [105] for references), as it is known that prolonged azole treatment can result in resistance [106,
599 107]. As well established, development of resistance would cause higher rates of treatment failure,
600 therefore implying an even more relevant role for azole persistence in *A. fumigatus* infections. Of
601 course, much more research is required to reach this conclusion, and we exhort the fungal research
602 community to consider and investigate this phenomenon to clarify this important matter.

603

604 **MATERIAL and METHODS**

605 ***A. fumigatus* strains and culture conditions.**

606 All isolates utilized in the course of this study are listed in Tables S1 and S8. Briefly, information
607 about the common laboratory strains used can be found in [108], the isolates from Paul Dyer
608 collection are described in [109] and the collection of isolates from the area of Manchester are
609 described in [69]. The third collection of isolates was collected at the TAU medical centre (Tel-Aviv,
610 Israel), these strains were characterized for their antifungal resistance profile and *cyp51A* genotype.

611 Isolates were routinely grown on Potato Dextrose Agar (PDA, Oxoid) for 72 hours to obtain fresh
612 spores for each experiment. *Aspergillus* Minimal Medium (AMM) was prepared following a standard
613 recipe [110]. Sabouraud (Oxoid) and yeast extract glucose (YAG, 2%, 0.5% yeast extract, 1.7% agar,
614 1X trace elements) media were used in specific experiments.

615 To evaluate persister growth and determine the MIC, isolates were grown on RPMI-1640 (Sigma)
616 with 35 g/L MOPS (Alfa Aesar) and 2% glucose, pH 7.

617 Galactosaminogalactan (GAG) was obtained from the *A. fumigatus* Δ*ku80* strain, grown 2-day in 1.5L
618 brian fermenter at room temperature. GAG isolation and purification was carried out as previously
619 described [111]. Briefly, the medium supernatant was collected by filtration and was adjusted to pH
620 3 by addition of 100 µl 12 M HCl per 100 ml supernatant. Two volumes of precooled ethanol (4°C)
621 were added and GAG was precipitated for 3 h at 4°C. The precipitate was collected by centrifugation
622 for 20 min at 5,000 g at 4°C and subsequently washed twice with 1/10 of the culture volume of 200
623 mM NaCl for 1 h under agitation (100 rpm). GAG was dialyzed against tap water and twice against
624 purified water (24 h each) and finally lyophilized to dryness and stored at ambient temperature.

625 **Evaluation of persistence and determination of MICs**.

626 To determine persistence using the disc assay, 4×10^4 conidia of each isolate was evenly spread on a
627 solidified RPMI plate (1.5% agar) and 10 µl of 0.8 mg/mL voriconazole or 3.2 mg/mL itraconazole
628 (Acros Organics) was added to a Whatman 6 mm antibiotic assay disc which was placed in the
629 middle of the plate. For *in vitro* treatment with adjuvant and combinatorial drugs, the agents were
630 added to the RPMI medium at the final concentration detailed in each section. Plates were
631 incubated for 5 days at 37 °C.

632 Minimum inhibitory concentrations (MICs) were calculated using the broth microdilution method
633 according to the EUCAST E.Def. 9.3 instructions [112]. 2.5×10^4 conidia were used in each well.

634 **Evaluation of the conidial survival to voriconazole fungicidal action**

635 To calculate the number of conidia that survived after exposure to high concentration of azoles, full
636 contents of the wells containing the highest concentration of each drug (8 µg/mL) in the broth
637 dilution assays were plated after 48-72 hours incubation on PDA and further incubated for 24-48 h at
638 37 °C.

639 Microscopic analysis was used to investigate the survival of strains upon withdrawal of voriconazole
640 at single cell level. 1.5×10^4 conidia of each strain were inoculated in 300 µL of RPMI in the presence
641 of 8 µg/mL voriconazole (European Pharmacopoeia, -EP- Reference Standard, Merck) and incubated
642 for 48 hours at 37 °C with occasional shaking. The strains were then centrifuged for 4000 RPM for 5
643 minutes, the media discarded and the conidia resuspended in 2 mL filtered PBS. This wash was
644 repeated three times in total before the conidia were resuspended in 600 µL of drug free RPMI. 300
645 µL of each suspension, approximately 7.5×10^3 conidia, was added into wells of a 96 well plate. The
646 wells were then imaged for 72 hours, every 2 hours, on a Nikon Eclipse Ti microscope, using a Nikon
647 CFI Plan Fluor ELWD 20x/0.45na objective, and captured with a Hamamatsu ORCA-FLASH4.0 LT+
648 camera (Hamamatsu Photonics) and manipulated using NIS-Elements AR 5.11.01 (Nikon). A video
649 was prepared using Fiji [113].

650 Microscopy to observe growth at supra-MIC conditions was done in a THUNDER Imager Live Cell
651 microscope, with a HC PL FLUOTAR L 20x/0.40 DRY objective. Images were captured using a Leica-
652 DFC9000GTC-VSC13067 camera and the Las X (Leica application suite) v 3.7 software.

653 To construct the killing curved, the isolates were inoculated in 10 mL of RPMI containing 4 µg/mL
654 voriconazole. Aliquots for each culture were taken at the time of inoculation (100 µL) and every 24
655 hours (1 mL). The aliquots were spun at 16,000 ×g for 5 minutes, resupended in 1 mL PBS and
656 vortexed. This was repeated twice to wash off the drug. Finally, conidia were resuspended in 1 mL

657 PBS and a fraction plated on PDA plates (50 µL at time 0h, 100 µL at 24h and 1 mL for 48, 72 and 96
658 h). The experiment was repeated three times.

659 To calculate the percentage of germinating conidia, the wells of broth dilution assays containing 2X,
660 3X MIC and the maximum drug concentration (8 µg/mL) were stained (after reading the MIC) with
661 10 µg/mL of Calcofluor White (Sigma) for 5 minutes. The entire wells were imaged with a THUNDER
662 Imager Live Cell microscope, using a HC PL FLUOTAR L 20x/0.40 DRY objective, filter conditions:
663 EX:375-435 DCC:455 EM:450-490, a Leica-DFC9000GTC-VSC13067 camera and the Las X (Leica
664 application suite) v 3.7 software. Merged images were analysed using FIJI [113]. Briefly, the merged
665 images were converted to 8-bit, a threshold was set for the images so that the conidia and germlings
666 could be detected over the background (20 to 255). The option analyse particle was then executed,
667 setting a minimum size of 0.04 $inches^2$ (which was found to exclude resting conidia). Wells
668 containing the maximum concentration of the drug, where only resting conidia can be found, were
669 used to set the background level of detection for each isolate (consisting of aggregates of conidia,
670 impurities and carry over conidiophores from the inoculum). The percentage of germinated
671 conidia/short hyphae was calculated as: (number of counted particles per well – number of counted
672 particles in max drug)/25000 (inoculum).

673 **Nucleic acid isolation**

674 For DNA extraction, 10^6 spores of each *A. fumigatus* isolate were grown overnight on liquid
675 *Aspergillus* minimal medium, filtered through Miracloth paper (Merck), snap frozen and ground in
676 constant presence of liquid nitrogen. Subsequently, DNA was extracted using a standard CTAB
677 method.

678 For RNA extraction, *A. fumigatus* isolates were grown on 0.45 µm pore nylon membranes (GE
679 Healthcare) placed on RPMI plates and incubated 1 day (without drug) or 5 days (with voriconazole
680 in a disc). Mycelia were scratched using a spatula and immediately frozen and grounded in liquid
681 nitrogen. Subsequently, RNA was extracted and purified with the Plant RNeasy Mini Kit (Qiagen)
682 following the manufacturer's instructions for filamentous fungi, and using on-column DNase
683 treatment.

684 For fungal burden calculations in *Galleria mellonella*, DNA was extracted from decapitated larvae
685 using the DNeasy Blood & Tissue Kit (Qiagen) following the manufacturer's instruction for animal
686 tissue, with overnight incubation at 56 °C.

687 ***Galleria mellonella* infection**

688 Sixth-stage instar larval *G. mellonella* moths were purchased from R.J.Mous Livebait (Eigen Haard,
689 The Netherlands). Randomly selected groups of 250-350 mg of weight larvae were injected in the
690 last left proleg with 5 µL of a 2×10^6 conidia/mL suspension (10^4 conidia/larva) of the correspondent
691 *Aspergillus fumigatus* isolate using Hamilton syringe. 2 hours after infection, relevant groups were
692 injected in the last right proleg with 5 µL of a suspension containing 1600 µg/mL (8 µg/larvae)
693 voriconazole. A PBS control group was subjected to the same treatment, but without fungal
694 infection.

695 To detect the fungal burden, 500-ng portions of DNA extracted from each larva were subjected to
696 qPCR using the SensiMic SybR Green kit (Bioline). Forward (5′-ACTTCCGCAATGGACGTTAC-3′) and
697 reverse (5′-GGATGTTGTTGGGAATCCAC-3') primers were used to amplify the *A. fumigatus* β-tubulin
698 gene (AFUA_7G00250). The primers designed to amplify the Elongation factor 1-Alpha (Ef-1a) were
699 as follows: forward (5′- AACCTCCTTACAGTGAATCC-3′) and reverse (5′- ATGTTATCTCCGTGCCAG-
700 3′). Standard curves were calculated using different concentrations of fungal and larval gDNA pure
701 template. Negative controls containing no template DNA were subjected to the same procedure to
702 exclude or detect any possible contamination. Three technical replicates were prepared for each
703 sample. qPCRs were performed using a CFX96 Real-Time System (Bio-rad) with the following thermal
704 cycling parameters: 95°C for 10 min and 40 cycles of 95°C for 15 s and 58°C for 15 s and 72°C for 15
705 s. The fungal burden was calculated by normalizing the number of fungal genome equivalents (i.e.,
706 the number of copies of the tubulin gene) to the larval genome equivalents in the sample (i.e., the
707 number of copies of the a Ef-1a gene), as we have reported before [114].

708 **RNA sequencing (RNA-seq)**

709 Total RNA was submitted to the Genomic Technologies Core Facility (GTCF) at the University of
710 Manchester, UK. Quality and integrity of the RNA samples were assessed using a 4200 TapeStation
711 (Agilent Technologies) and then libraries generated using the Illumina® Stranded mRNA Prep.
712 Ligation kit (Illumina, Inc.) according to the manufacturer's protocol. Briefly, total RNA (typically
713 0.025-1ug) was used as input material from which polyadenylated mRNA was purified using poly-T,
714 oligo-attached, magnetic beads. Next, the mRNA was fragmented under elevated temperature and
715 then reverse transcribed into first strand cDNA using random hexamer primers and in the presence
716 of Actinomycin D (thus improving strand specificity whilst mitigating spurious DNA-dependent
717 synthesis). Following removal of the template RNA, second strand cDNA was then synthesized to
718 yield blunt-ended, double-stranded cDNA fragments. Strand specificity was maintained by the
719 incorporation of deoxyuridine triphosphate (dUTP) in place of dTTP to quench the second strand
720 during subsequent amplification. Following a single adenine (A) base addition, adapters with a
721 corresponding, complementary thymine (T) overhang were ligated to the cDNA fragments. Pre-index

722 anchors were then ligated to the ends of the double-stranded cDNA fragments to prepare them for
723 dual indexing. A subsequent PCR amplification step was then used to add the index adapter
724 sequences to create the final cDNA library. The adapter indices enabled the multiplexing of the
725 libraries, which were pooled prior to cluster generation using a cBot instrument. The loaded flow-cell
726 was then paired-end sequenced (76 + 76 cycles, plus indices) on an Illumina HiSeq4000 instrument.
727 Finally, the output data was demultiplexed and BCL-to-Fastq conversion performed using Illumina's
728 bcl2fastq software, version 2.20.0.422

729 **RNA-seq analysis**

730 Unmapped paired-reads of 76bp from the Illumina HiSeq4000 sequencer were checked using a
731 quality control pipeline consisting of FastQC v0.11.3
732 (http://www.bioinformatics.babraham.ac.uk/projects/fastqc/) and FastQ Screen v0.13.0
733 (https://www.bioinformatics.babraham.ac.uk/projects/fastq_screen/).
734 The reads were trimmed to remove any adapter or poor quality sequence using Trimmomatic v0.39
735 [115]; reads were truncated at a sliding 4bp window, starting 5', with a mean quality <Q20, and
736 removed if the final length was less than 35bp. Additional flags included: 'ILLUMINACLIP:./Truseq3-
737 PE-2_Nextera-PE.fa:2:30:10 SLIDINGWINDOW:4:20 MINLEN:35'.
738 The filtered reads were mapped either to the *Aspergillus fumigatus* A1163 reference sequence
739 (GCA_000150145.1/ASM15014v1) downloaded from the Ensembl Genomes Fungi v44 [116] or PD-
740 104 a *de novo* assembled genome, using STAR v5.3a [117]. For A1163 reference the genome index
741 was created using the GTF gene annotation also from Ensembl Genomes Fungi v44. For the PD-104
742 reference GTF gene annotation was generated as described below. A suitable flag for the read
743 length (--sjdbOverhang 75) was used. '--quantMode GeneCounts' was used to generate read counts
744 in genes.
745 Subsequently, PD-104 reads were aligned to the recently generated pan-genome [62] using Salmon
746 v1.6.0 (additional parameters for salmon quant: --gcBias (corrects for any GC biases in samples) -l ISR
747 (inward / stranded / reverse read pairs)).
748 Normalisation and differential expression analysis was performed using DESeq2 v1.34.0 [118] on R
749 v4.1.2 (R Core Team. 2021. R: A Language and Environment for Statistical Computing.
750 https://www.R-project.org/). Log fold change shrinkage was applied using the lfcShrink function
751 along with the "apeglm" algorithm [119].

752 **DNA sequencing (Illumina DNA Prep)**

753 Genomic DNA was submitted to the Genomic Technologies Core Facility (GTCF) at the University of
754 Manchester. Sequencing libraries were generated using on-bead tagmentation chemistry with the
755 llumina® DNA Prep, (M) Tagmentation Kit (Illumina, Inc.) according to the manufacturer's protocol.

756 Briefly, bead-linked transposomes were used to mediate the simultaneous fragmentation of gDNA
757 (100-500ng) and the addition of Illumina sequencing primers. Next, reduced-cycle PCR amplification
758 was used to amplify sequencing ready DNA fragments and to add the indices and adapters. Finally,
759 sequencing-ready fragments were washed and pooled prior to paired-end sequencing (151 + 151
760 cycles, plus indices) on an Illumina NextSeq500 instrument. Finally, the output data were
761 demultiplexed (allowing one mismatch) and BCL-to-Fastq conversion performed using Illumina's
762 bcl2fastq software, version 2.20.0.422.
763 The RNA data is stored in Array Express, accession E-MTAB-11547
764 (https://www.ebi.ac.uk/arrayexpress/experiments/E-MTAB-11547).
765 **Method for de novo genome assembly of genomes (PD-104 as example):**
766 Unmapped paired-end reads of 149bp from an Illumina NextSeq500 sequencer were checked using a
767 quality control pipeline consisting of FastQC v0.11.3
768 (http://www.bioinformatics.babraham.ac.uk/projects/fastqc/) and FastQ Screen v0.13.0
769 (https://www.bioinformatics.babraham.ac.uk/projects/fastq_screen/).
770 The reads were trimmed to remove any adapter or poor quality sequence using Trimmomatic v0.39
771 [115]. Within the first or last 30bp of a read bases were removed if quality was <30. A sliding 2bp
772 window, starting 5', scanned the reads and truncated at a window with a mean quality <Q20. Reads
773 were removed if the final length was less than 100bp. Additional flags included:
774 'ILLUMINACLIP:../Truseq3_Nextera-PE.fa:2:30:10 LEADING:30 TRAILING:30 SLIDINGWINDOW:2:20
775 MINLEN:100'.
776 Genome assembly was performed using Megahit v1.2.9 [120], using the flag '--no-mercy'. This
777 resulted in 799 contigs, total 28659847 bp, min 202 bp, max 401152 bp, avg 35869 bp, N50 97740
778 bp. In comparison A1163 has 55 contigs total 29205420 bp.
779 Quast v5.0.2 [121] was used to determine the quality of the assembly. An example of the PD-104
780 results can be found in Table S10.
781 ProtHint v2.5.0 and GeneMark-EP+ v4.68_lic [122] were used for gene annotation. ProtHint was
782 used to generate the evidence for coding genes in combination with fungal protein download from
783 OrthoDb v10. ProtHint generates two main outputs: `prothint.gff` a GFF file with all reported hints
784 (introns, starts and stops), and `evidence.gff` high confidence subset of `prothint.gff` which is
785 suitable for the GeneMark-EP Plus mode. GeneMark-EP+ was used to generate a GTF file of
786 candidate genes for the PD-104 assembly. Additional parameters were set '--max_intron 200 --
787 max_intergenic 100000 --min_contig=1000 --fungus'.
788 In order to determine the function of the novel genes, initially a reciprocal best hit strategy was used
789 comparing protein sequence from PD-104 (using the GeneMark Perl script

790 'get_sequence_from_GTF.pl' with the GTF file and assembled contigs) and A1163 (proteins
791 downloaded from Ensembl Genomes Fungi release 51:
792 http://ftp.ensemblgenomes.org/pub/fungi/release-
793 51/fasta/aspergillus_fumigatusa1163/pep/Aspergillus_fumigatusa1163.ASM15014v1.pep.all.fa.gz).
794 The best match method was run using proteinortho v6.0.31 [123], which by default uses the
795 program Diamond v2.0.13 [124] to identify protein matches ('-p=diamond'). The flag '-sim=1' was set
796 to obtain best reciprocal matches only.

797 **Construction of Phylogenetic tree:**

798 Pre-alignment, the reference Af293 genome [125] was masked to remove low-complexity regions
799 using RepeatMasker (http://www.repeatmasker.org/) v.4.1.2-p1 and the Dfam repeat database
800 [126] release 3.5. Quality-checked DNA sequencing reads from the recently generated pan-genome
801 study [62] were combined with the reads generated from this study and underwent alignment to the
802 masked reference Af293 genome, using BWA-MEM [127] v.0.7.17-r1188. Alignment files were then
803 converted to the sorted BAM format using SAMtools [128] v.1.10. Variant calling was then
804 performed with GATK HaplotypeCaller [129] v.4.0. All variant calls with a genotype quality less than
805 50 were removed and low-confidence SNPs were converted to missing data if they met one of the
806 follow criteria: DP<10|| RMSMappingQuality<40.0|| QualByDepth<2.0||
807 FisherStrand>60.0|| ABHom<0.9. Each newly generated VCF file was then compressed,
808 indexed and then merged into a single file using VCFtools [130] v.0.1.16. This data was then
809 converted into a relaxed interleaved Phylip format using vcf2phylip [131] v2.8 and RAxML [132]
810 v.8.2.12, under rapid bootstrap analysis using 1,000 replicates with the GTRCAT model, was
811 employed to generate maximum-likelihood phylogenies to test whether persistence is lineage-
812 specific. Phylogenetic trees with overlaying metadata were generated using iTOL [133] v.6.5.4.
813
814

815 **ACKNOWLEGDGEMENTS**

816 We are deeply grateful to Prof Paul Dyer, who kindly gifted to us the collection of isolates that have
817 been used in this study. We would like to thank Diego Megías and Clara Martín at ISCIII for their help
818 with the microscopy. We are also grateful to Michael Bottery for relevant conversations about
819 bacterial tolerance and persistence. We acknowledge the use of the Genomic Technologies Facility
820 (Faculty of Biology Medicine and Health, University of Manchester) for the DNA and RNA
821 sequencing. Help and support from members of MFIG and LRIM is greatly appreciated.

822 JA is funded by an Atracción de Talento Modalidad 1 (020-T1/BMD-200) contract of the Madrid
823 Regional Government (CAM). JS has been funded by a BSAC Scholarship (bsac-2016-0049). CV was

824 funded by FAPESP (2108/00715-3 and 2020/01131-5). GHG has been funded by FAPESP
825 (2016/07870-9 and 2021/04977-5) and CNPq (301058/2019-9 and 404735/2018-5). SG was co-
826 funded by the NIHR Manchester Research Centre and the Fungal Infection Trust.
827

828 **DATA AVAILABILITY**

829 Transcriptomic data is available in Array Express
830 (https://www.ebi.ac.uk/arrayexpress/experiments/E-MTAB-11547). All raw data is available upon
831 reasonable request.

832
833
834
835
836
837
838
839
840
841
842
843

844 **REFERENCES**

845 1. Latgé, J.-P. and G. Chamilos, *Aspergillus fumigatus and Aspergillosis in 2019.* Clinical
846 Microbiology Reviews, 2019. **33**(1) DOI: 10.1128/cmr.00140-18.
847 2. Perfect, J.R., *The antifungal pipeline: a reality check.* Nat Rev Drug Discov, 2017. **16**(9): p.
848 603-616 DOI: 10.1038/nrd.2017.46.
849 3. Ruping, M.J., J.J. Vehreschild, and O.A. Cornely, *Antifungal treatment strategies in high risk*
850 *patients.* Mycoses, 2008. **51 Suppl 2**: p. 46-51 DOI: 10.1111/j.1439-0507.2008.01572.x.
851 4. Koehler, P., et al., *Defining and managing COVID-19-associated pulmonary aspergillosis: the*
852 *2020 ECMM/ISHAM consensus criteria for research and clinical guidance.* The Lancet
853 Infectious Diseases, 2021. **21**(6): p. e149-e162 DOI: 10.1016/s1473-3099(20)30847-1.
854 5. Marr, K.A., et al., *Aspergillosis Complicating Severe Coronavirus Disease.* Emerging Infectious
855 Diseases, 2021. **27**(1): p. 18-25 DOI: 10.3201/eid2701.202896.
856 6. Helleberg, M., M. Steensen, and M.C. Arendrup, *Invasive aspergillosis in patients with severe*
857 *COVID-19 pneumonia.* Clinical Microbiology and Infection, 2021. **27**(1): p. 147-148 DOI:
858 10.1016/j.cmi.2020.07.047.
859 7. Lowes, D., et al., *Predictors of mortality in chronic pulmonary aspergillosis.* Eur Respir J,
860 2017. **49**(2) DOI: 10.1183/13993003.01062-2016.
861 8. Brown, G.D., et al., *Hidden killers: human fungal infections.* Sci Transl Med, 2012. **4**(165): p.
862 165rv13 DOI: 10.1126/scitranslmed.3004404.

863 9. Ballou, L., *Fungal diseases deserve our attention.* Nature Microbiology Community, 2017.
864 http://go.nature.com/2jlKFYZ.
865 10. Fisher, M.C., et al., *Worldwide emergence of resistance to antifungal drugs challenges*
866 *human health and food security.* Science, 2018. **360**(6390): p. 739-742 DOI:
867 10.1126/science.aap7999.
868 11. Verweij, P.E., et al., *International expert opinion on the management of infection caused by*
869 *azole-resistant Aspergillus fumigatus.* Drug Resist Updat, 2015. **21-22**: p. 30-40 DOI:
870 10.1016/j.drup.2015.08.001.
871 12. Lestrade, P.P., et al., *Voriconazole Resistance and Mortality in Invasive Aspergillosis: A*
872 *Multicenter Retrospective Cohort Study.* Clin Infect Dis, 2019. **68**(9): p. 1463-1471 DOI:
873 10.1093/cid/ciy859.
874 13. Meis, J.F., et al., *Clinical implications of globally emerging azole resistance in Aspergillus*
875 *fumigatus.* Philos Trans R Soc Lond B Biol Sci, 2016. **371**(1709) DOI: 10.1098/rstb.2015.0460.
876 14. Galiger, C., et al., *Assessment of efficacy of antifungals against Aspergillus fumigatus: value*
877 *of real-time bioluminescence imaging.* Antimicrob Agents Chemother, 2013. **57**(7): p. 3046-
878 59 DOI: 10.1128/AAC.01660-12.
879 15. Heo, S.T., et al., *Changes in In Vitro Susceptibility Patterns of Aspergillus to Triazoles and*
880 *Correlation With Aspergillosis Outcome in a Tertiary Care Cancer Center, 1999–2015.* Clinical
881 Infectious Diseases, 2017. **65**(2): p. 216-225 DOI: 10.1093/cid/cix297.
882 16. Leong, J.M., et al., *Antibiotic tolerance.* PLOS Pathogens, 2020. **16**(10) DOI:
883 10.1371/journal.ppat.1008892.
884 17. Levinson, T., et al., *Impact of tolerance to fluconazole on treatment response in Candida*
885 *albicans bloodstream infection.* Mycoses, 2020. **64**(1): p. 78-85 DOI: 10.1111/myc.13191.
886 18. Brauner, A., et al., *Distinguishing between resistance, tolerance and persistence to antibiotic*
887 *treatment.* Nature Reviews Microbiology, 2016. **14**(5): p. 320-330 DOI:
888 10.1038/nrmicro.2016.34.
889 19. Balaban, N.Q., et al., *Definitions and guidelines for research on antibiotic persistence.* Nature
890 Reviews Microbiology, 2019. **17**(7): p. 441-448 DOI: 10.1038/s41579-019-0196-3.
891 20. Meylan, S., I.W. Andrews, and J.J. Collins, *Targeting Antibiotic Tolerance, Pathogen by*
892 *Pathogen.* Cell, 2018. **172**(6): p. 1228-1238 DOI: 10.1016/j.cell.2018.01.037.
893 21. Rosenberg, A., et al., *Antifungal tolerance is a subpopulation effect distinct from resistance*
894 *and is associated with persistent candidemia.* Nature Communications, 2018. **9**(1) DOI:
895 10.1038/s41467-018-04926-x.
896 22. Martos, A.I., et al., *Evaluation of the Etest method for susceptibility testing of Aspergillus spp.*
897 *and Fusarium spp. to three echinocandins.* Med Mycol, 2010. **48**(6): p. 858-61 DOI:
898 10.3109/13693781003586943.
899 23. Lass-Florl, C., et al., *Antifungal susceptibility testing in Aspergillus spp. according to EUCAST*
900 *methodology.* Med Mycol, 2006. **44**(Supplement_1): p. S319-S325 DOI:
901 10.1080/13693780600779401.
902 24. Bleichrodt, R.J., et al., *Cell Wall Composition Heterogeneity between Single Cells in*
903 *Aspergillus fumigatus Leads to Heterogeneous Behavior during Antifungal Treatment and*
904 *Phagocytosis.* mBio, 2020. **11**(3) DOI: 10.1128/mBio.03015-19.
905 25. Wagener, J. and V. Loiko, *Recent Insights into the Paradoxical Effect of Echinocandins.*
906 Journal of Fungi, 2017. **4**(1) DOI: 10.3390/jof4010005.
907 26. Valero, C., et al., *The Caspofungin Paradoxical Effect is a Tolerant "Eagle Effect" in the*
908 *Filamentous Fungal Pathogen Aspergillus fumigatus.* mBio, 2022 DOI: 10.1128/mbio.00447-
909 22.
910 27. Aruanno, M., E. Glampedakis, and F. Lamoth, *Echinocandins for the Treatment of Invasive*
911 *Aspergillosis: from Laboratory to Bedside.* Antimicrobial Agents and Chemotherapy, 2019.
912 **63**(8) DOI: 10.1128/aac.00399-19.

913 28. Gheith, S., et al., *In vitro susceptibility to amphotericin B, itraconazole, voriconazole,*
914 *posaconazole and caspofungin of Aspergillus spp. isolated from patients with haematological*
915 *malignancies in Tunisia.* Springerplus, 2014. **3**: p. 19 DOI: 10.1186/2193-1801-3-19.
916 29. Geißel, B., et al., *Azole-induced cell wall carbohydrate patches kill Aspergillus fumigatus.*
917 Nature Communications, 2018. **9**(1) DOI: 10.1038/s41467-018-05497-7.
918 30. Majoros, L. and G. Kardos, *Fungicidal Activity of Azole Antifungal Agents.* Anti-Infective
919 Agents in Medicinal Chemistry, 2008. **7**(2): p. 118-125 DOI: 10.2174/187152108783954623.
920 31. Manavathu, E.K., J.L. Cutright, and P.H. Chandrasekar, *Organism-Dependent Fungicidal*
921 *Activities of Azoles.* Antimicrobial Agents and Chemotherapy, 1998. **42**(11): p. 3018-3021
922 DOI: 10.1128/aac.42.11.3018.
923 32. Wang, F., et al., *Transcription in fungal conidia before dormancy produces phenotypically*
924 *variable conidia that maximize survival in different environments.* Nature Microbiology,
925 2021. **6**(8): p. 1066-1081 DOI: 10.1038/s41564-021-00922-y.
926 33. Gefen, O., et al., *TDtest: easy detection of bacterial tolerance and persistence in clinical*
927 *isolates by a modified disk-diffusion assay.* Sci Rep, 2017. **7**: p. 41284 DOI:
928 10.1038/srep41284.
929 34. Gonzalez-Jimenez, I., et al., *Are Point Mutations in HMG-CoA Reductases (Hmg1 and Hmg2)*
930 *a Step towards Azole Resistance in Aspergillus fumigatus?* Molecules, 2021. **26**(19) DOI:
931 10.3390/molecules26195975.
932 35. Zhang, J., et al., *Evolution of cross-resistance to medical triazoles in Aspergillus fumigatus*
933 *through selection pressure of environmental fungicides.* Proceedings of the Royal Society B:
934 Biological Sciences, 2017. **284**(1863) DOI: 10.1098/rspb.2017.0635.
935 36. Windels, E.M., et al., *Bacterial persistence promotes the evolution of antibiotic resistance by*
936 *increasing survival and mutation rates.* The ISME Journal, 2019. **13**(5): p. 1239-1251 DOI:
937 10.1038/s41396-019-0344-9.
938 37. Sebastian, J., et al., *De Novo Emergence of Genetically Resistant Mutants of Mycobacterium*
939 *tuberculosis from the Persistence Phase Cells Formed against Antituberculosis Drugs In Vitro.*
940 Antimicrobial Agents and Chemotherapy, 2017. **61**(2) DOI: 10.1128/aac.01343-16.
941 38. Suh, M.-J., et al., *Development stage-specific proteomic profiling uncovers small, lineage*
942 *specific proteins most abundant in the Aspergillus fumigatus conidial proteome.* Proteome
943 Science, 2012. **10**(1) DOI: 10.1186/1477-5956-10-30.
944 39. Mowat, E., et al., *Phase-dependent antifungal activity against Aspergillus fumigatus*
945 *developing multicellular filamentous biofilms.* Journal of Antimicrobial Chemotherapy, 2008.
946 **62**(6): p. 1281-1284 DOI: 10.1093/jac/dkn402.
947 40. Yu, J.S.L., et al., *Microbial communities form rich extracellular metabolomes that foster*
948 *metabolic interactions and promote drug tolerance.* Nature Microbiology, 2022. **7**(4): p. 542-
949 555 DOI: 10.1038/s41564-022-01072-5.
950 41. Day, A.M. and J. Quinn, *Stress-Activated Protein Kinases in Human Fungal Pathogens.*
951 Frontiers in Cellular and Infection Microbiology, 2019. **9** DOI: 10.3389/fcimb.2019.00261.
952 42. Hagiwara, D., et al., *Signaling pathways for stress responses and adaptation in Aspergillus*
953 *species: stress biology in the post-genomic era.* Bioscience, Biotechnology, and Biochemistry,
954 2016. **80**(9): p. 1667-1680 DOI: 10.1080/09168451.2016.1162085.
955 43. Manfiolli, A.O., et al., *Aspergillus fumigatus High Osmolarity Glycerol Mitogen Activated*
956 *Protein Kinases SakA and MpkC Physically Interact During Osmotic and Cell Wall Stresses.*
957 Frontiers in Microbiology, 2019. **10** DOI: 10.3389/fmicb.2019.00918.
958 44. Takahashi, H., et al., *Global gene expression reveals stress-responsive genes in Aspergillus*
959 *fumigatus mycelia.* BMC Genomics, 2017. **18**(1) DOI: 10.1186/s12864-017-4316-z.
960 45. Berman, J. and D.J. Krysan, *Drug resistance and tolerance in fungi.* Nat Rev Microbiol, 2020
961 DOI: 10.1038/s41579-019-0322-2.

46. Cowen, L.E., et al., *Harnessing Hsp90 function as a powerful, broadly effective therapeutic strategy for fungal infectious disease.* Proceedings of the National Academy of Sciences, 2009. **106**(8): p. 2818-2823 DOI: 10.1073/pnas.0813394106.
47. Lamoth, F., et al., *Antifungal activity of compounds targeting the Hsp90-calcineurin pathway against various mould species.* Journal of Antimicrobial Chemotherapy, 2015. **70**(5): p. 1408-1411 DOI: 10.1093/jac/dku549.
48. Juvvadi, P.R., F. Lamoth, and W.J. Steinbach, *Calcineurin as a multifunctional regulator: Unraveling novel functions in fungal stress responses, hyphal growth, drug resistance, and pathogenesis.* Fungal Biology Reviews, 2014. **28**(2-3): p. 56-69 DOI: 10.1016/j.fbr.2014.02.004.
49. Sestari, S.J., et al., *Inhibition of protein kinase A affects Paracoccidioides lutzii dimorphism.* International Journal of Biological Macromolecules, 2018. **113**: p. 1214-1220 DOI: 10.1016/j.ijbiomac.2018.03.023.
50. Chen, S.C.A., R.E. Lewis, and D.P. Kontoyiannis, *Direct effects of non-antifungal agents used in cancer chemotherapy and organ transplantation on the development and virulence of Candida and Aspergillus species.* Virulence, 2014. **2**(4): p. 280-295 DOI: 10.4161/viru.2.4.16764.
51. Weichert, M., et al., *Functional Coupling between the Unfolded Protein Response and Endoplasmic Reticulum/Golgi Ca2+-ATPases Promotes Stress Tolerance, Cell Wall Biosynthesis, and Virulence of Aspergillus fumigatus.* mBio, 2020. **11**(3) DOI: 10.1128/mBio.01060-20.
52. Istvan, E.S., *Structural Mechanism for Statin Inhibition of HMG-CoA Reductase.* Science, 2001. **292**(5519): p. 1160-1164 DOI: 10.1126/science.1059344.
53. Qiao, J., et al., *Antifungal activity of statins against Aspergillus species.* Med Mycol, 2007. **45**(7): p. 589-93 DOI: 10.1080/13693780701397673.
54. Silva, L.V., et al., *Milbemycins: More than Efflux Inhibitors for Fungal Pathogens.* Antimicrobial Agents and Chemotherapy, 2012. **57**(2): p. 873-886 DOI: 10.1128/aac.02040-12.
55. Esquivel, B.D., et al., *Characterization of the Efflux Capability and Substrate Specificity of Aspergillus fumigatus PDR5-like ABC Transporters Expressed in Saccharomyces cerevisiae.* mBio, 2020. **11**(2) DOI: 10.1128/mBio.00338-20.
56. Gonzalez-Jimenez, I., et al., *A Cyp51B Mutation Contributes to Azole Resistance in Aspergillus fumigatus.* Journal of Fungi, 2020. **6**(4) DOI: 10.3390/jof6040315.
57. Rybak, J.M., et al., *Mutations in hmg1, Challenging the Paradigm of Clinical Triazole Resistance in Aspergillus fumigatus.* mBio, 2019. **10**(2) DOI: 10.1128/mBio.00437-19.
58. Furukawa, T., et al., *The negative cofactor 2 complex is a key regulator of drug resistance in Aspergillus fumigatus.* Nat Commun, 2020. **11**(1): p. 427 DOI: 10.1038/s41467-019-14191-1.
59. Hulsen, T., J. de Vlieg, and W. Alkema, *BioVenn - a web application for the comparison and visualization of biological lists using area-proportional Venn diagrams.* BMC Genomics, 2008. **9**: p. 488 DOI: 10.1186/1471-2164-9-488.
60. Amos, B., et al., *VEuPathDB: the eukaryotic pathogen, vector and host bioinformatics resource center.* Nucleic Acids Research, 2022. **50**(D1): p. D898-D911 DOI: 10.1093/nar/gkab929.
61. Peyrusson, F., et al., *Intracellular Staphylococcus aureus persisters upon antibiotic exposure.* Nature Communications, 2020. **11**(1) DOI: 10.1038/s41467-020-15966-7.
62. Rhodes, J., et al., *Population genomics confirms acquisition of drug-resistant Aspergillus fumigatus infection by humans from the environment.* Nature Microbiology, 2022 DOI: 10.1038/s41564-022-01091-2.
63. Szklarczyk, D., et al., *The STRING database in 2021: customizable protein-protein networks, and functional characterization of user-uploaded gene/measurement sets.* Nucleic Acids Res, 2021. **49**(D1): p. D605-D612 DOI: 10.1093/nar/gkaa1074.

1013 64. Rossi, N.A., I. El Meouche, and M.J. Dunlop, *Forecasting cell fate during antibiotic exposure*
1014 *using stochastic gene expression.* Communications Biology, 2019. **2**(1) DOI: 10.1038/s42003-
1015 019-0509-0.
1016 65. Urbaniec, J., et al., *Phenotypic heterogeneity in persisters: a novel 'hunker' theory of*
1017 *persistence.* FEMS Microbiology Reviews, 2022. **46**(1) DOI: 10.1093/femsre/fuab042.
1018 66. Fraczek, M.G., et al., *The cdr1B efflux transporter is associated with non-cyp51a-mediated*
1019 *itraconazole resistance in Aspergillus fumigatus* Journal of Antimicrobial Chemotherapy,
1020 2013. **68**(7): p. 1486-1496 DOI: 10.1093/jac/dkt075.
1021 67. Bamford, N.C., et al., *Sph3 Is a Glycoside Hydrolase Required for the Biosynthesis of*
1022 *Galactosaminogalactan in Aspergillus fumigatus.* Journal of Biological Chemistry, 2015.
1023 **290**(46): p. 27438-27450 DOI: 10.1074/jbc.M115.679050.
1024 68. Lee, M.J., et al., *Deacetylation of Fungal Exopolysaccharide Mediates Adhesion and Biofilm*
1025 *Formation.* mBio, 2016. **7**(2) DOI: 10.1128/mBio.00252-16.
1026 69. Bromley, M.J., et al., *Occurrence of azole-resistant species of Aspergillus in the UK*
1027 *environment.* J Glob Antimicrob Resist, 2014. **2**(4): p. 276-279 DOI:
1028 10.1016/j.jgar.2014.05.004.
1029 70. Gonzalez-Jimenez, I., et al., *Multiresistance to Nonazole Fungicides in Aspergillus fumigatus*
1030 *TR34/L98H Azole-Resistant Isolates.* Antimicrobial Agents and Chemotherapy, 2021. **65**(9)
1031 DOI: 10.1128/aac.00642-21.
1032 71. Forastiero, A., et al., *In vivo efficacy of voriconazole and posaconazole therapy in a novel*
1033 *invertebrate model of Aspergillus fumigatus infection.* International Journal of Antimicrobial
1034 Agents, 2015. **46**(5): p. 511-517 DOI: 10.1016/j.ijantimicag.2015.07.007.
1035 72. Gomez-Lopez, A., et al., *An invertebrate model to evaluate virulence in Aspergillus*
1036 *fumigatus: The role of azole resistance.* Medical Mycology, 2014. **52**(3): p. 311-319 DOI:
1037 10.1093/mmy/myt022.
1038 73. Jemel, S., et al., *In Vivo Efficacy of Voriconazole in a Galleria mellonella Model of Invasive*
1039 *Infection Due to Azole-Susceptible or Resistant Aspergillus fumigatus Isolates.* Journal of
1040 Fungi, 2021. **7**(12) DOI: 10.3390/jof7121012.
1041 74. Hobby, G.L., K. Meyer, and E. Chaffee, *Observations on the Mechanism of Action of Penicillin.*
1042 Experimental Biology and Medicine, 1942. **50**(2): p. 281-285 DOI: 10.3181/00379727-50-
1043 13773.
1044 75. Bigger, J., *Treatment of Staphylococcal Infections with Penicillin by Intermittent Sterilisation.*
1045 The Lancet, 1944. **244**(6320): p. 497-500 DOI: 10.1016/s0140-6736(00)74210-3.
1046 76. Cohen, Nadia R., Michael A. Lobritz, and James J. Collins, *Microbial Persistence and the Road*
1047 *to Drug Resistance.* Cell Host & Microbe, 2013. **13**(6): p. 632-642 DOI:
1048 10.1016/j.chom.2013.05.009.
1049 77. Huemer, M., et al., *Antibiotic resistance and persistence—Implications for human health and*
1050 *treatment perspectives.* EMBO reports, 2020. **21**(12) DOI: 10.15252/embr.202051034.
1051 78. LaFleur, M.D., C.A. Kumamoto, and K. Lewis, *Candida albicans Biofilms Produce Antifungal-*
1052 *Tolerant Persister Cells.* Antimicrobial Agents and Chemotherapy, 2006. **50**(11): p. 3839-3846
1053 DOI: 10.1128/aac.00684-06.
1054 79. Hobman, T.C., et al., *Fungal persister cells: The basis for recalcitrant infections?* PLOS
1055 Pathogens, 2018. **14**(10) DOI: 10.1371/journal.ppat.1007301.
1056 80. Kowalski, C.H., et al., *Fungal biofilm architecture produces hypoxic microenvironments that*
1057 *drive antifungal resistance.* Proceedings of the National Academy of Sciences, 2020. **117**(36):
1058 p. 22473-22483 DOI: 10.1073/pnas.2003700117.
1059 81. Wilmaerts, D., et al., *General Mechanisms Leading to Persister Formation and Awakening.*
1060 Trends in Genetics, 2019. **35**(6): p. 401-411 DOI: 10.1016/j.tig.2019.03.007.
1061 82. Orman, M.A. and M.P. Brynildsen, *Dormancy Is Not Necessary or Sufficient for Bacterial*
1062 *Persistence.* Antimicrobial Agents and Chemotherapy, 2013. **57**(7): p. 3230-3239 DOI:
1063 10.1128/aac.00243-13.

1064 83. Wakamoto, Y., et al., *Dynamic Persistence of Antibiotic-Stressed Mycobacteria.* Science,
1065 2013. **339**(6115): p. 91-95 DOI: 10.1126/science.1229858.
1066 84. Claudi, B., et al., *Phenotypic Variation of Salmonella in Host Tissues Delays Eradication by*
1067 *Antimicrobial Chemotherapy.* Cell, 2014. **158**(4): p. 722-733 DOI: 10.1016/j.cell.2014.06.045.
1068 85. Stapels, D.A.C., et al., *Salmonella persisters undermine host immune defenses during*
1069 *antibiotic treatment.* Science, 2018. **362**(6419): p. 1156-1160 DOI: 10.1126/science.aat7148.
1070 86. Li, P., et al., *Delicate Metabolic Control and Coordinated Stress Response Critically Determine*
1071 *Antifungal Tolerance of Candida albicans Biofilm Persisters.* Antimicrobial Agents and
1072 Chemotherapy, 2015. **59**(10): p. 6101-6112 DOI: 10.1128/aac.00543-15.
1073 87. Monteiro, M.C., et al., *A New Approach to Drug Discovery: High-Throughput Screening of*
1074 *Microbial Natural Extracts against Aspergillus fumigatus Using Resazurin* Journal of
1075 Biomolecular Screening, 2012. **17**(4): p. 542-549 DOI: 10.1177/1087057111433459.
1076 88. Hillmann, F., E. Shekhova, and O. Kniemeyer, *Insights into the cellular responses to hypoxia*
1077 *in filamentous fungi.* Current Genetics, 2015. **61**(3): p. 441-455 DOI: 10.1007/s00294-015-
1078 0487-9.
1079 89. Barber, A.E., et al., *Aspergillus fumigatus pan-genome analysis identifies genetic variants*
1080 *associated with human infection.* Nature Microbiology, 2021. **6**(12): p. 1526-1536 DOI:
1081 10.1038/s41564-021-00993-x.
1082 90. Manuse, S., et al., *Bacterial persisters are a stochastically formed subpopulation of low-*
1083 *energy cells.* PLOS Biology, 2021. **19**(4) DOI: 10.1371/journal.pbio.3001194.
1084 91. Zalis, E.A., et al., *Stochastic Variation in Expression of the Tricarboxylic Acid Cycle Produces*
1085 *Persister Cells.* mBio, 2019. **10**(5) DOI: 10.1128/mBio.01930-19.
1086 92. El Meouche, I., Y. Siu, and M.J. Dunlop, *Stochastic expression of a multiple antibiotic*
1087 *resistance activator confers transient resistance in single cells.* Scientific Reports, 2016. **6**(1)
1088 DOI: 10.1038/srep19538.
1089 93. Pu, Y., et al., *Enhanced Efflux Activity Facilitates Drug Tolerance in Dormant Bacterial Cells.*
1090 Molecular Cell, 2016. **62**(2): p. 284-294 DOI: 10.1016/j.molcel.2016.03.035.
1091 94. Fontaine, T., et al., *Galactosaminogalactan, a New Immunosuppressive Polysaccharide of*
1092 *Aspergillus fumigatus.* PLoS Pathogens, 2011. **7**(11) DOI: 10.1371/journal.ppat.1002372.
1093 95. Speth, C., et al., *Galactosaminogalactan (GAG) and its multiple roles in Aspergillus*
1094 *pathogenesis.* Virulence, 2019. **10**(1): p. 976-983 DOI: 10.1080/21505594.2019.1568174.
1095 96. Fisher, R.A., B. Gollan, and S. Helaine, *Persistent bacterial infections and persister cells.*
1096 Nature Reviews Microbiology, 2017. **15**(8): p. 453-464 DOI: 10.1038/nrmicro.2017.42.
1097 97. Mondon, P., et al., *Heteroresistance to fluconazole and voriconazole in Cryptococcus*
1098 *neoformans.* Antimicrob Agents Chemother, 1999. **43**(8): p. 1856-61 DOI:
1099 10.1128/AAC.43.8.1856.
1100 98. Yamazumi, T., et al., *Characterization of Heteroresistance to Fluconazole among Clinical*
1101 *Isolates of Cryptococcus neoformans.* Journal of Clinical Microbiology, 2003. **41**(1): p. 267-
1102 272 DOI: 10.1128/jcm.41.1.267-272.2003.
1103 99. Varma, A. and K.J. Kwon-Chung, *Heteroresistance of Cryptococcus gattii to Fluconazole.*
1104 Antimicrobial Agents and Chemotherapy, 2010. **54**(6): p. 2303-2311 DOI:
1105 10.1128/aac.00153-10.
1106 100. Stone, N.R.H., et al., *Dynamic ploidy changes drive fluconazole resistance in human*
1107 *cryptococcal meningitis.* Journal of Clinical Investigation, 2019. **129**(3): p. 999-1014 DOI:
1108 10.1172/jci124516.
1109 101. Barsh, G.S., et al., *A non-canonical RNA degradation pathway suppresses RNAi-dependent*
1110 *epimutations in the human fungal pathogen Mucor circinelloides.* PLOS Genetics, 2017. **13**(3)
1111 DOI: 10.1371/journal.pgen.1006686.
1112 102. Ferreira, G.F. and D.A. Santos, *Heteroresistance and fungi.* Mycoses, 2017. **60**(9): p. 562-568
1113 DOI: 10.1111/myc.12639.

1114 103. Sionov, E., et al., *Heteroresistance to Fluconazole in Cryptococcus neoformans Is Intrinsic and*
1115 *Associated with Virulence.* Antimicrobial Agents and Chemotherapy, 2009. **53**(7): p. 2804-
1116 2815 DOI: 10.1128/aac.00295-09.
1117 104. Todd, R.T. and A. Selmecki, *Expandable and reversible copy number amplification drives*
1118 *rapid adaptation to antifungal drugs.* eLife, 2020. **9** DOI: 10.7554/eLife.58349.
1119 105. Windels, E.M., et al., *Antibiotics: Combatting Tolerance To Stop Resistance.* mBio, 2019.
1120 **10**(5) DOI: 10.1128/mBio.02095-19.
1121 106. Tashiro, M., et al., *Correlation between Triazole Treatment History and Susceptibility in*
1122 *Clinically Isolated Aspergillus fumigatus.* Antimicrobial Agents and Chemotherapy, 2012.
1123 **56**(9): p. 4870-4875 DOI: 10.1128/Aac.00514-12.
1124 107. Kamei, K., et al., *High detection rate of azole-resistant Aspergillus fumigatus after treatment*
1125 *with azole antifungal drugs among patients with chronic pulmonary aspergillosis in a single*
1126 *hospital setting with low azole resistance.* Medical Mycology, 2020 DOI:
1127 10.1093/mmy/myaa052.
1128 108. Bertuzzi, M., et al., *On the lineage of Aspergillus fumigatus isolates in common laboratory*
1129 *use.* Medical Mycology, 2021. **59**(1): p. 7-13 DOI: 10.1093/mmy/myaa075.
1130 109. Swilaiman, S.S., et al., *Global Sexual Fertility in the Opportunistic Pathogen Aspergillus*
1131 *fumigatus and Identification of New Supermater Strains.* J Fungi (Basel), 2020. **6**(4) DOI:
1132 10.3390/jof6040258.
1133 110. Moreno, M.A., et al., *Culture conditions for zinc- and pH-regulated gene expression studies in*
1134 *Aspergillus fumigatus.* Int Microbiol, 2007. **10**(3): p. 187-92.
1135 111. Gressler, M., et al., *Definition of the Anti-inflammatory Oligosaccharides Derived From the*
1136 *Galactosaminogalactan (GAG) From Aspergillus fumigatus.* Frontiers in Cellular and Infection
1137 Microbiology, 2019. **9** DOI: 10.3389/fcimb.2019.00365.
1138 112. Arendrup, M.C., et al., *EUCAST technical note on isavuconazole breakpoints for Aspergillus,*
1139 *itraconazole breakpoints for Candida and updates for the antifungal susceptibility testing*
1140 *method documents.* Clinical Microbiology and Infection, 2016. **22**(6): p. 571.e1-571.e4 DOI:
1141 10.1016/j.cmi.2016.01.017.
1142 113. Schindelin, J., et al., *Fiji: an open-source platform for biological-image analysis.* Nature
1143 Methods, 2012. **9**(7): p. 676-682 DOI: 10.1038/nmeth.2019.
1144 114. Scott, J., et al., *Pseudomonas aeruginosa-Derived Volatile Sulfur Compounds Promote Distal*
1145 *Aspergillus fumigatus Growth and a Synergistic Pathogen-Pathogen Interaction That*
1146 *Increases Pathogenicity in Co-infection.* Front Microbiol, 2019. **10**: p. 2311 DOI:
1147 10.3389/fmicb.2019.02311.
1148 115. Bolger, A.M., M. Lohse, and B. Usadel, *Trimmomatic: a flexible trimmer for Illumina sequence*
1149 *data.* Bioinformatics, 2014. **30**(15): p. 2114-2120 DOI: 10.1093/bioinformatics/btu170.
1150 116. Howe, K.L., et al., *Ensembl Genomes 2020—enabling non-vertebrate genomic research.*
1151 Nucleic Acids Research, 2020. **48**(D1): p. D689-D695 DOI: 10.1093/nar/gkz890.
1152 117. Dobin, A., et al., *STAR: ultrafast universal RNA-seq aligner.* Bioinformatics, 2013. **29**(1): p. 15-
1153 21 DOI: 10.1093/bioinformatics/bts635.
1154 118. Love, M.I., W. Huber, and S. Anders, *Moderated estimation of fold change and dispersion for*
1155 *RNA-seq data with DESeq2.* Genome Biology, 2014. **15**(12) DOI: 10.1186/s13059-014-0550-8.
1156 119. Zhu, A., et al., *Heavy-tailed prior distributions for sequence count data: removing the noise*
1157 *and preserving large differences.* Bioinformatics, 2019. **35**(12): p. 2084-2092 DOI:
1158 10.1093/bioinformatics/bty895.
1159 120. Li, D., et al., *MEGAHIT: an ultra-fast single-node solution for large and complex*
1160 *metagenomics assembly via succinct de Bruijn graph.* Bioinformatics, 2015. **31**(10): p. 1674-
1161 1676 DOI: 10.1093/bioinformatics/btv033.
1162 121. Gurevich, A., et al., *QUAST: quality assessment tool for genome assemblies.* Bioinformatics,
1163 2013. **29**(8): p. 1072-1075 DOI: 10.1093/bioinformatics/btt086.

1164 122. Brůna, T., A. Lomsadze, and M. Borodovsky, *GeneMark-EP+: eukaryotic gene prediction with*
1165 *self-training in the space of genes and proteins.* NAR Genomics and Bioinformatics, 2020.
1166 **2**(2) DOI: 10.1093/nargab/lqaa026.
1167 123. Lechner, M., et al., *Proteinortho: Detection of (Co-)orthologs in large-scale analysis.* BMC
1168 Bioinformatics, 2011. **12**(1) DOI: 10.1186/1471-2105-12-124.
1169 124. Buchfink, B., C. Xie, and D.H. Huson, *Fast and sensitive protein alignment using DIAMOND.*
1170 Nature Methods, 2014. **12**(1): p. 59-60 DOI: 10.1038/nmeth.3176.
1171 125. Nierman, W.C., et al., *Genomic sequence of the pathogenic and allergenic filamentous*
1172 *fungus Aspergillus fumigatus.* Nature, 2005. **438**(7071): p. 1151-1156 DOI:
1173 10.1038/nature04332.
1174 126. Hubley, R., et al., *The Dfam database of repetitive DNA families.* Nucleic Acids Research,
1175 2016. **44**(D1): p. D81-D89 DOI: 10.1093/nar/gkv1272.
1176 127. Heng, L., *Aligning sequence reads, clone sequences and assembly contigs with BWA-MEM.*
1177 arXiv:1303.3997, 2013 DOI:
1178 https://doi.org/10.48550/arXiv.1303.3997.
1179 128. Li, H., et al., *The Sequence Alignment/Map format and SAMtools.* Bioinformatics, 2009.
1180 **25**(16): p. 2078-2079 DOI: 10.1093/bioinformatics/btp352.
1181 129. van Arkel, A.L.E., et al., *COVID-19–associated Pulmonary Aspergillosis.* American Journal of
1182 Respiratory and Critical Care Medicine, 2020. **202**(1): p. 132-135 DOI: 10.1164/rccm.202004-
1183 1038LE.
1184 130. Danecek, P., et al., *The variant call format and VCFtools.* Bioinformatics, 2011. **27**(15): p.
1185 2156-2158 DOI: 10.1093/bioinformatics/btr330.
1186 131. Ortiz, E.M., *vcf2phylip v2.0: convert a VCF matrix into several matrix formats for*
1187 *phylogenetic analysis. (v2.0).* in *Zenodo*. 2019.
1188 132. Stamatakis, A., *RAxML-VI-HPC: maximum likelihood-based phylogenetic analyses with*
1189 *thousands of taxa and mixed models.* Bioinformatics, 2006. **22**(21): p. 2688-2690 DOI:
1190 10.1093/bioinformatics/btl446.
1191 133. Ciccarelli, F.D., et al., *Toward Automatic Reconstruction of a Highly Resolved Tree of Life.*
1192 Science, 2006. **311**(5765): p. 1283-1287 DOI: 10.1126/science.1123061.
1193 134. Supek, F., et al., *REVIGO Summarizes and Visualizes Long Lists of Gene Ontology Terms.* PLoS
1194 ONE, 2011. **6**(7) DOI: 10.1371/journal.pone.0021800.

1195

1196

1197

1198

1199 **FIGURE CAPTIONS**

1200 **Figure 1. Certain *Aspergillus fumigatus* isolates display persistence to voriconazole.**

1201 **A)** In disc-diffusion assays (10 µL of 0.8 mg/mL voriconazole), the susceptible isolate ATCC46645
1202 never grew any colony in the inhibition halo, the resistant control (RC) isolate grew up to the edge of
1203 the disc. The strain PD-256 always grew numerous colonies that neatly covered the halo, and the
1204 persister isolate PD-104 was consistently able to grow a few small colonies. Plates were incubated
1205 for 5 days at 37°C. **B)** Inspection of the wells of a broth dilution assay under the microscope 72 hours
1206 after inoculation revealed that the non-persister isolates ATCC and PD-60 displayed only limited
1207 microscopic growth at the MIC concentration, and all conidia remained ungerminated at higher
1208 concentrations. In contrast, the persister strains PD-9 and PD-104 showed noticeable microscopic
1209 growth up to three fold (3x) the MIC concentration. Scale bar= 132.5 µm. **C)** Full content of the well
1210 containing the maximum concentration of voriconazole (8 µg/mL) was plated on rich media PDA
1211 plates and colony forming units (CFUs) counted 48 hours after inoculation. Persister isolates grew
1212 significantly more CFUs than non-persister isolates (PD-9 VS ATC46645C p=0.002 and PD-104 VS
1213 ATCC46645 p=0.0331), demonstrating that these strains remain viable upon azole treatment for a
1214 longer period. Three independent experiments with three biological replicates were performed, the
1215 graph represents the means and SD, and data was analysed using the Brown-Forsythe and Welch
1216 ANOVA test with Dunnett's multiple comparisons. **D)** A survival curve in the presence of 4 µg/mL of
1217 voriconazole revealed that, whilst non-persister strains lost viability very rapidly, the persister
1218 isolates had the characteristic bi-phasic reduction in viability, showing that a sub-population of the
1219 persister isolates remained viable for a longer period. The experiment was done in biological
1220 duplicates with two technical replicates, the graph represents the means and SD.

1221 **Figure 2. *Aspergillus fumigatus* persistence does not depend on the morphological stage, but**
1222 **seems to be determined by the growth media**.

1223 **A)** Conidia of the different isolates were inoculated and incubated for 8 or 16 hours before the disc
1224 containing voriconazole (10 µL of 0.8 mg/mL) was added to the RPMI plate. At 8 hours, when conidia
1225 have germinated, the persister isolates PD-9 and PD-104 were still able to grow small colonies in the
1226 inhibition halo, whilst the non-persister strains were not. At 16 hours, when conidia have already
1227 formed hyphae, the background growth made impossible to distinguish colonies in PD-9, but a clear
1228 one could be detected in PD-104. **B)** On *Aspergillus* minimal medium (MM), the persister isolate PD-
1229 104 was able to form colonies in the halo, but the non-persister strain ATCC was not. **C)** On rich
1230 media PDA and Sabouraud (Sab) all isolates were able to form conidia in the halo. **D)** This happened
1231 even the MIC of all isolates was the same in commonly assayed RPMI and the rich media Sab.

1232 **Figure 3. *Aspergillus fumigatus* persistence is not influenced by stress, with the exception of**
1233 **hypoxia, and cannot be eliminated with adjuvant or combinatorial treatments.**

1234 **A)** Hypoxia was the only stress that could prevent persistence, whilst neither oxidative (H_2O_2), cell
1235 wall (SDS or CFW) or osmotic (NaCl) stress influenced persistence. **B)** Hypoxia completely eradicated
1236 persistence also on the rich medium YAG for ATCC, PD-60 and PD-9, but only reduced persistence for
1237 the PD-104. **C)** The use of adjuvant drugs could not prevent persistence. **D)** Combinatorial treatment
1238 with amphotericin-B and caspofungin did not prevent persistence. All plates were incubated with 10
1239 µL of 0.8 mg/mL voriconazole added to the disc and the specific condition (stress, adjuvant or
1240 combinatorial drug) as described in the text. Plates were incubated for 5 days at 37°C. All plates and
1241 conditions were repeated in two independent experiments.

1242 **Figure 4. RNA-seq analysis reveals potential causes of persistence**.

1243 **A)** Schematic representation of the conditions assayed, the comparisons made and the number of
1244 genes identified, as detailed in the text. In addition, the sites of sampling for the no drug (plate
1245 without voriconazole disc), low drug (light green circle at mid-distance of the inhibition halo) and
1246 persistence (colonies inside the inhibition halos) conditions are shown. **B-E** The most significantly
1247 upregulated GO biological processes are shown using the REVINGO tool for GO data visualization
1248 [134]. The full list of upregulated GO terms can be found in Tables S2-S5 and Table 2. **B**) PD-104
1249 Persister only genes (aligned to the A1163 genome), **C)** all genes upregulated in Persistence (aligned
1250 to the pangenome), **D)** PD-104 Persister only genes, (aligned to the pangenome) and **E)** genes that
1251 are most upregulated in persistence compared to normal response to the drug.

1252 **Figure 5. External addition of GAG potentiates persistence in the isolate PD-104**.

1253 **A)** Addition of GAG does not change the MIC of the isolates. **B)** Representative merges of 87 photos
1254 to cover the whole well of broth dilution assays. The fungal material was stained with calcofluor
1255 white. Representative wells of PD-104 with and without GAG at 2X the MIC are shown **C)** Counting of
1256 germinated conidia/short hyphae in the entire wells of 2X (left) and 3X (right) MIC of broth dilution
1257 assays. External addition of GAG significantly increased the number of germlings in PD-104 from
1258 1.09% to 2.80%, p=0.0267 at 2X MIC and from 0.41% to 0.75% p=0.038, two-tailed unpaired t-test.
1259 Two independent experiments with two technical replicates were performed. The graphs represent
1260 the means and SD. **D)** Plating of the entire content of wells containing 4 µg/mL of voriconazole
1261 shows that external addition of GAG significantly increased the number of viable PD-104 cells that
1262 can be recovered 48 hours after inoculation (p=0.0437, one way ANOVA with Tukey's multiple
1263 comparisons). Two independent experiments with three biological replicates were performed. The
1264 graph represents the means and SD.

1265 **Figure 6. Persister isolates do not form a distinct lineage.**

1266 The genomes of newly sequenced persister and non-persister isolates, as characterised in this study
1267 (Table S9), distributed scattered when included in the previously generated phylogenetic tree [62].
1268 Therefore, persistence is not a feature that has evolved in a particular lineage.

1269 **Figure 7. Voriconazole eliminates persister isolates less efficiently than non-persister strains in a**
1270 ***Galleria mellonella* infection model.**

1271 **A)** Survival curve of larvae infected with 10^4 conidia of the isolates ATCC, PD-60 (non-persisters), PD-
1272 9 or PD-104 (persisters). All strains killed larvae at a similar rate, demonstrating that they are equally
1273 virulent. Three independent experiments were done with 15-20 larvae/isolate in each. **B)** Fungal
1274 burden was measured by qPCR 72 h after infection with 10^4 conidia. For all strains, fungal burden
1275 was greatly lower in larvae that had received a voriconazole treatment (8 µg/mL) that in those who
1276 had not. The reduction in burden was bigger in non-persister isolates than in persister isolates.

1277

1278 **Supplementary Figures**

1279 **Fig. S1.**

1280 Disc diffusion screening of the PD-47 collection of isolates (Table S1) on RPMI plate with 10 µL of 0.8
1281 mg/mL voriconazole. Only 5 isolates could grow colonies in the inhibition halos. Upon re-inoculation
1282 of the colonies of the halo, PD-254, PD-256 and PD-266 covered the entire plate. As explained in the
1283 text those strains were classified as resistant or heteroresistant. In contrast, PD-9 and PD-104 CoHs
1284 showed upon re-inoculation the same level of growth as the original isolates. These strains were
1285 classified as persisters.

1286 **Fig. S2.**

1287 Two CoHs from PD-9 and PD-104 were picked and sequentially passaged on PDA without drug. Every
1288 second passage the spores were inoculated in a new disc diffusion assay to check the level of
1289 resistance (diameter of the halo) and persistence (appearance of colonies in the halo). After 7
1290 passages both CoHs from both isolates showed the same level of persistence, demonstrating that
1291 this phenotype is stable.

1292 **Fig. S3.**

1293 Disc diffusion screening of the PD-47 collection of isolates. Three days after inoculation, the disc
1294 containing voriconazole (10 µL of 0.8 mg/mL) was substituted for another one containing *Aspergillus*
1295 minimal medium. A few colonies were able to grow colonies in the halos after the switch, suggesting

1296 that a few conidia remain viable. Only three strains PD-9 and PD-104 and PD-259 grew colonies
1297 before the switch. Of those, only PD-9 and PD-104 grew additional colonies after the switch.

1298 **Fig. S4.**

1299 Independent repetitions of the experiment shown in Figure 1B. The wells of 1X, 2X and 3X MIC of
1300 voriconazole for the isolates ATCC, PD-9, PD-60 and PD-104 were imaged under the microscope. The
1301 non-persister isolates ATCC and PD-60 only displayed limited microscopic growth at 1X MIC. In
1302 contrast, the persister isolates PD-9 and PD-104 displayed microscopic growth at 1X, 2X and 3X
1303 supra-MIC concentrations. Scale bar= 132.5 µm.

1304 **Fig. S5.**

1305 Disc diffusion screening of the PD-47 collection of isolates (Table S1) on RPMI plate with 10 µL of 3.2
1306 mg/mL itraconazole. Isolates RC (as expected) and PD-256 did not form an inhibition halo, reflecting
1307 that they are resistant to itraconazole. Isolates PD-104 and PD-266 could grow colonies in the halo.
1308 PD-104 formed upon re-inoculation a halo of the same size and similar number of CoHs as the
1309 original isolate, suggesting that it is persistence to itraconazole. The isolate PD-266 nearly covered
1310 the inhibition halo upon reinoculation, suggesting an increment in its MIC and therefore that it is
1311 likely heteroresistant to itraconazole, as previously described for voriconazole.

1312 **Fig. S6.**

1313 **A)** MICs of itraconazole and isavuconazole for the isolates ATCC, PD-9, PD-60 and PD-104, as
1314 calculated by broth dilution assay. **B)** The isolates PD-9 and PD-104 displayed some microscopic
1315 growth at 2X the MIC concentration for both azoles, whilst the isolates ATCC and PD-60 did not grow
1316 at all and only resting conidia could be found. **C)** The entire content of the wells containing the
1317 highest concentration (8 µg/mL) if each azole were inoculated on PDA plates and incubated for 48 h
1318 at 37 °C. A noticeable ratio of viable conidia were detected for the isolates PD-9 and PD-104. Each
1319 experiment was repeated twice independently. The graph represents the means and SD

1320 **Fig. S7.**

1321 **A)** A nylon membrane was placed on the RPMI plate. Conidia were inoculated on the membrane and
1322 the disc containing voriconazole (10 µL of 0.8 mg/mL) was also put on it. As in a normal disc diffusion
1323 assay, an inhibition halo was formed, inside of which the persister strain PD-104 was able to grow
1324 small colonies, but the non-persister strain A1160 was not. **B)** A network of interacting proteins was
1325 detected by STRING (p=1.84e-08) when using as query the 64 genes upregulated only in persistence
1326 in PD-104. Seventeen proteins related with metabolism formed a node, formed a node suggesting a
1327 specific metabolic response during persister growth. **C)** Within the 18 genes that were upregulated

1328 in all comparisons, a tight node of 6 interacting proteins, related with ergosterol production, was
1329 detected by STRING (p<1.0e-16).

1330 **Fig. S8.**

1331 **A)** Representative disc diffusion plates carried out with the collection of isolates from the TAU
1332 medical centre. Six isolates were able to form CoHs, which did upon reinoculation form halos of the
1333 same size (MIC did not increase) and create a similar number of CoHs. **B)** Resazurin was added to the
1334 broth dilution RPMI plate at a 0.002% (w/v) final concentration. The plate was incubated for 24
1335 hours in a Tecan Infinity M-Plex plate reader and fluorescence was measured every 30 minutes with
1336 an excitation wavelength of 544 nm and reading emission at 590 nm using the i-control 2.0 software.
1337 The read for each well at each time point was normalize as follows: (read well time X– read 8 µg/mL
1338 voriconazole time X)/read well at time 0. The time point with the best dynamic range of values in the
1339 1X, 2X and 3X MIC was found to be 20 hours, which was selected to determine the metabolic
1340 activity. A value of 0.1 was assigned as background and values above 1 were detected in sub-MIC
1341 (macroscopic growth). At 1X MIC, a slight metabolic activity could be detected for both the non-
1342 persister ATCC and the persister isolates PD-9 and PD-104. At 2X and 3X the MIC, slight metabolic
1343 activity could only be detected for the persister isolates. The experiment was performed once with
1344 two biological replicates, the graph represent the means and SEM.

1345 **Supplementary Files**

1346 **Table S1:** Collection of isolates used in this study.

1347 **Table S2:** Synonymous polymorphisms detected in the *cyp51B* gene of the isolates ATCC46645, PD-9,
1348 PD-60 and PD-104.

1349 **Table S3**: GO enrichment of genes regulated exclusively in Persistence (A1163 genome as reference).

1350 **Table S4:** GO enrichment of genes regulated in Persiter VS Low Drug (Pangenome as reference).

1351 **Table S5:** GO enrichment of genes regulated exclusively in Persistence (Pangenome as reference).

1352 **Table S6:** Proteins included in the STRING network (genes upregulated only in Persistence).

1353 **Table S7**: GO enrichment of genes regulated more in Persistence (Pangenome as reference).

1354 **Table S8:** Proteins included in the STRING network (genes upregulated more in Persistence).

1355 **Table S9:** List of environmental isolates in the UK collection. Identity of the sequenced genomes. List
1356 of the clinical isolates of the TAU collection.

1357 **Table S10:** Example of the Quast obtained to determine the quality of the assembly, using the PD-
1358 104 genome.

1359 **DataSet1:** RNA-seq results and analysis of the A1160 isolate grown in NoDrug and Low Drug.

1360 **DataSet2:** RNA-seq results and analysis of the PD-104 isolate grown in NoDrug, Low Drug and
1361 Persister, using the A1163 genome as reference for the alignment of reads.

1362 **DataSet3:** RNA-seq results and analysis of the PD-104 isolate grown in NoDrug, Low Drug and
1363 Persister, using the pangenome genome as reference for the alignment of reads.

1364 **Video S1:** The persister isolate PD-9 pre-incubated in voriconazole resumes growth when the drug is
1365 withdrawn.

1366 **Video S2** The persister isolate PD-104 pre-incubated in voriconazole resumes growth when the drug
1367 is withdrawn.

1368 **Video S3** The non-persister isolate ATCC46645 pre-incubated in voriconazole resumes growth when
1369 the drug is withdrawn.

Fig. 1

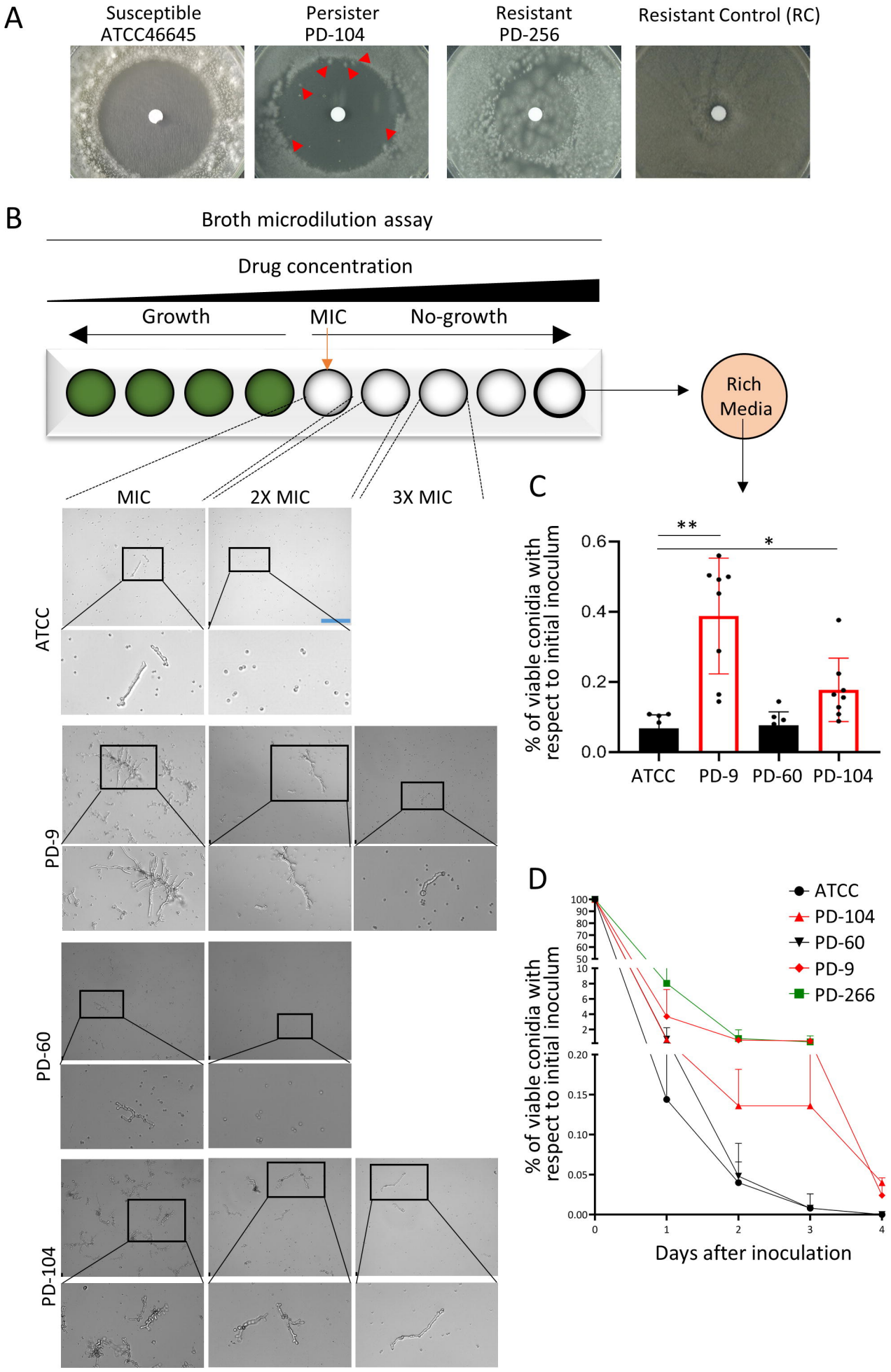
A
Susceptible
ATCC46645
Persister
PD-104
Resistant
PD-256
Resistant Control (RC)
B
Broth microdilution assay
Drug concentration
Growth
MIC
No-growth
Rich
Media
MIC
2X MIC
3X MIC
ATCC
PD-9
PD-60
PD-104
C
% of viable conidia with respect to initial inoculum
0.6
0.4
0.2
0.0
**
*
ATCC
PD-9
PD-60
PD-104
D
% of viable conidia with respect to initial inoculum
ATCC
PD-104
PD-60
PD-9
PD-266
Days after inoculation

Fig. 2

A

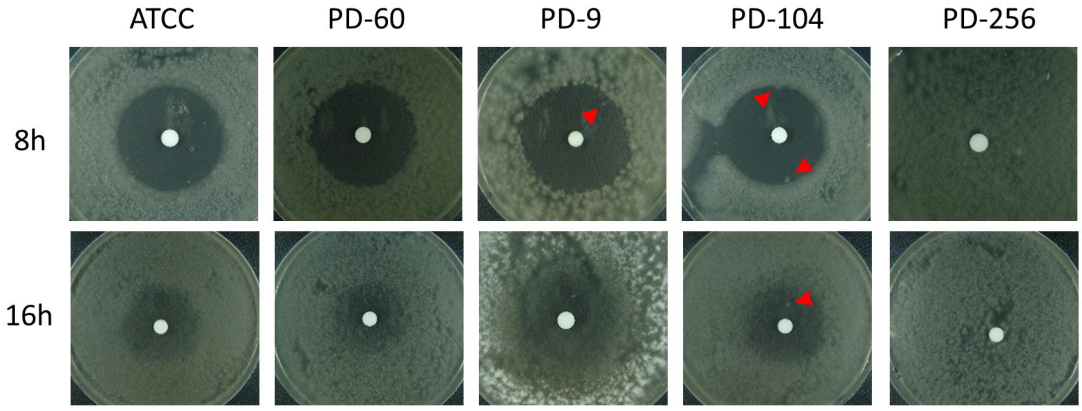

B

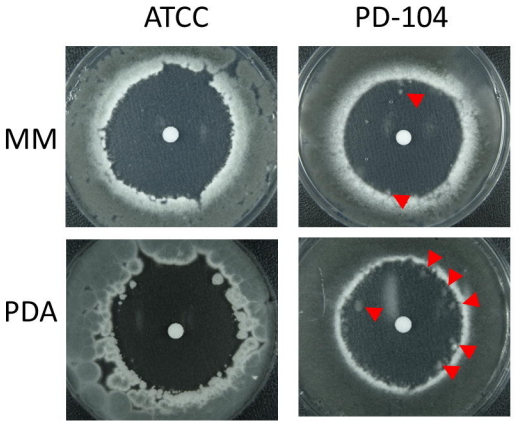

D

Voriconazole		
Isolate	MIC in RPMI	MIC in Sabouraud
ATCC	0.25	0.25
CEA10	0.25	0.25
PD-9	0.5	0.5
PD-104	1	1
PD-60	1	1
PD-266	8	8

C

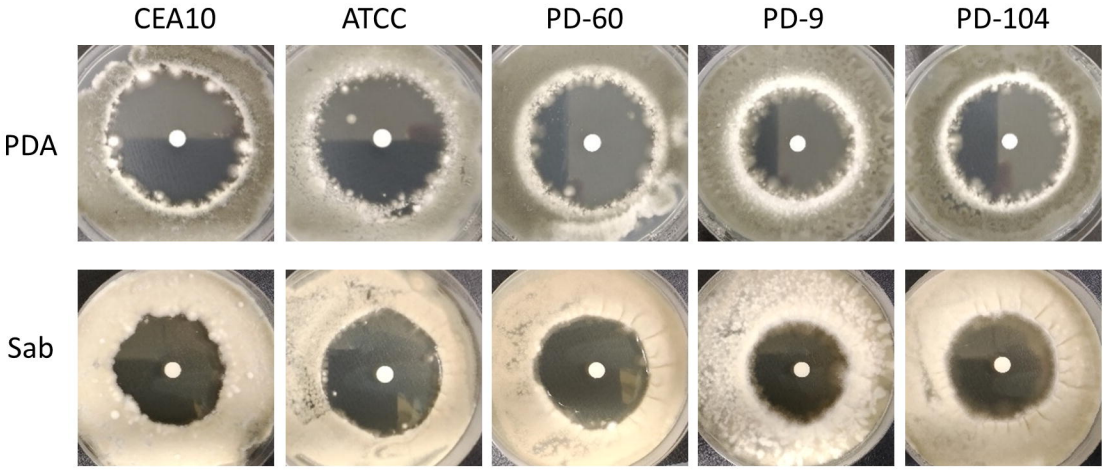

Fig. 3

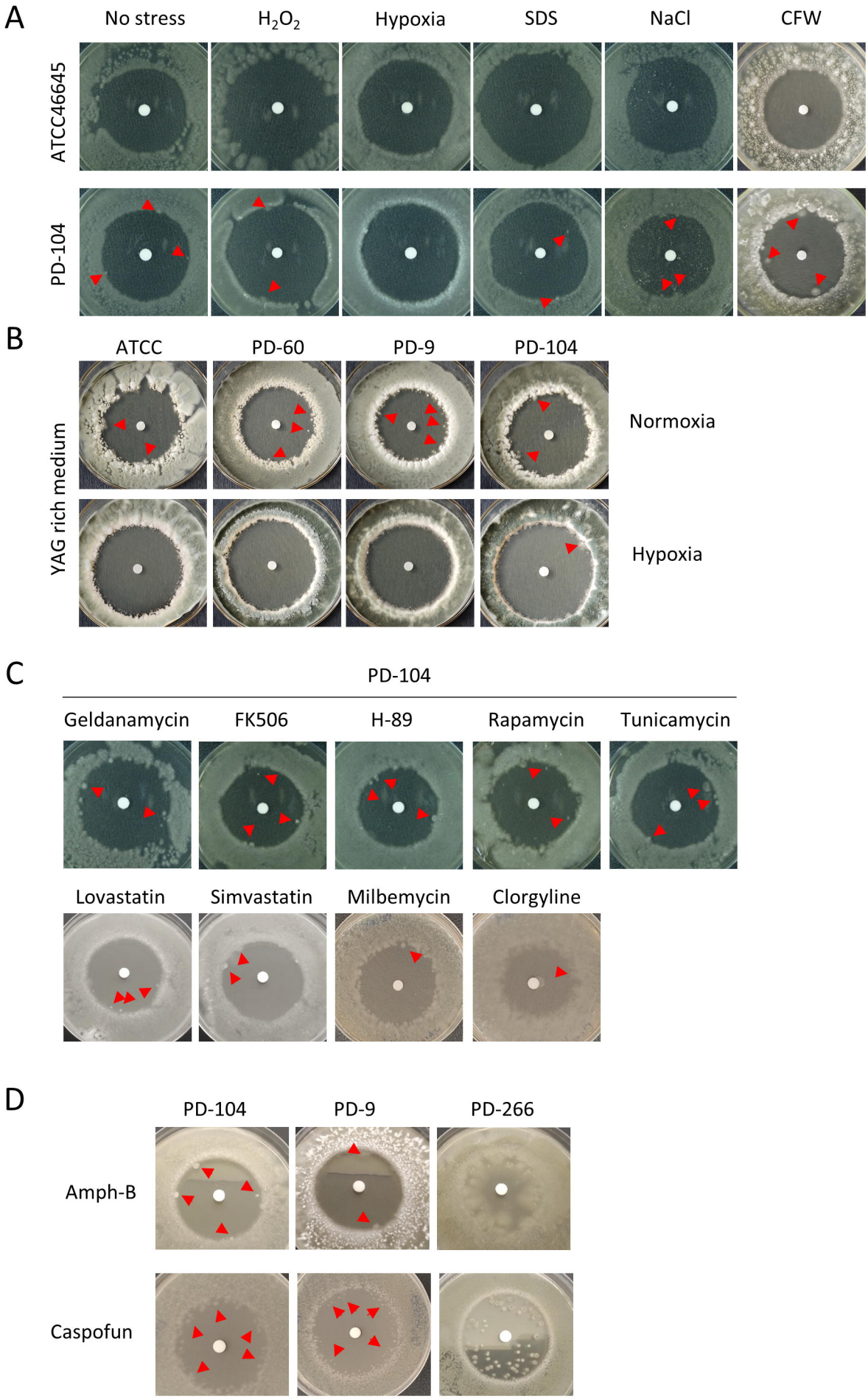
A
No stress
H_2O_2
Hypoxia
SDS
NaCl
CFW
ATCC46645
PD-104
B
ATCC
PD-60
PD-9
PD-104
YAG rich medium
Normoxia
Hypoxia
C
PD-104
Geldanamycin
FK506
H-89
Rapamycin
Tunicamycin
Lovastatin
Simvastatin
Milbemycin
Clorgyline
D
PD-104
PD-9
PD-266
Amph-B
Caspofun

Fig. 4

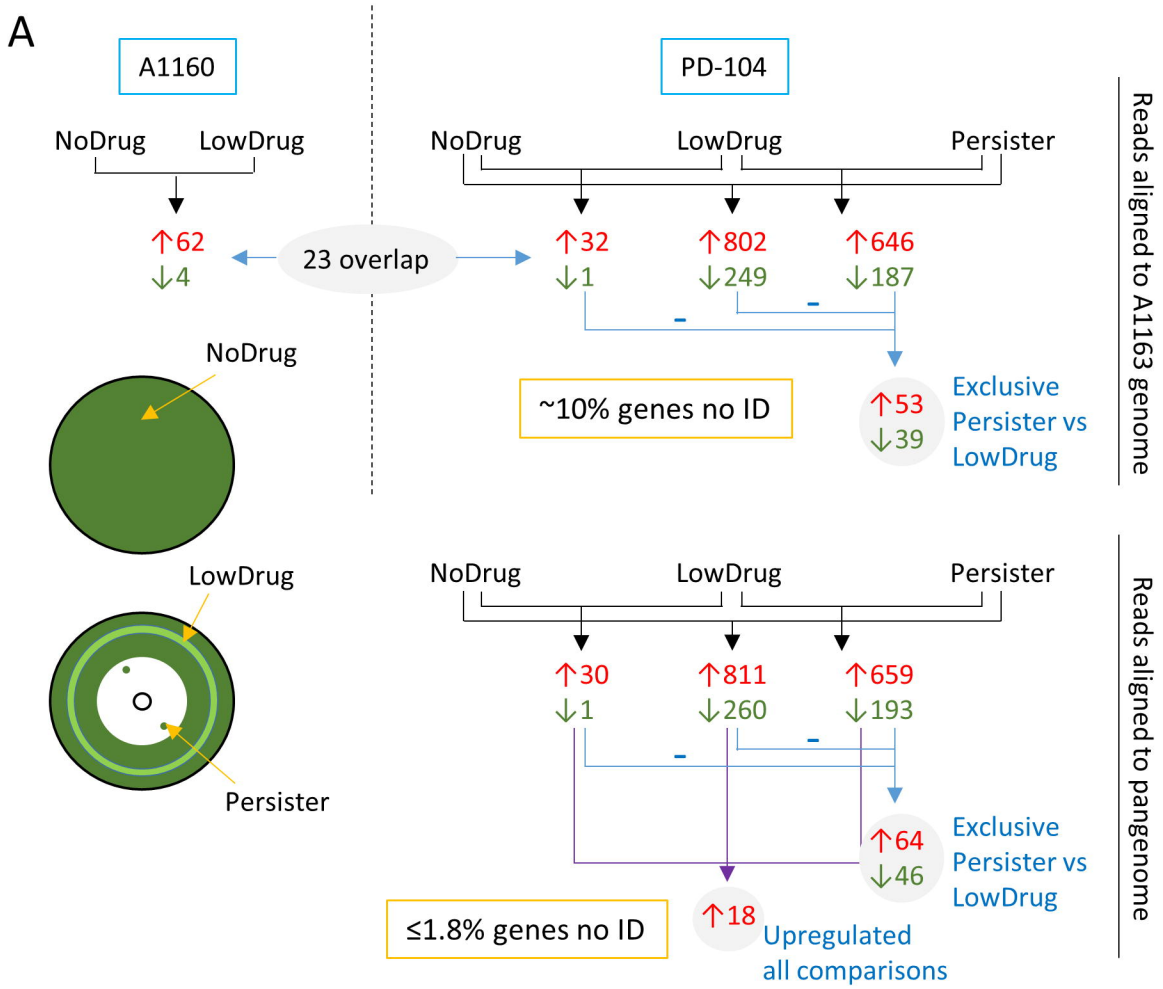
A
A1160
NoDrug
LowDrug
↑62
↓4
23 overlap
PD-104
NoDrug
LowDrug
Persister
↑32
↓1
↑802
↓249
↑646
↓187
~10% genes no ID
↑53
↓39
Exclusive Persister vs LowDrug
Reads aligned to A1163 genome
NoDrug
LowDrug
Persister
↑30
↓1
↑811
↓260
↑659
↓193
↑64
↓46
Exclusive Persister vs LowDrug
≤1.8% genes no ID
↑18
Upregulated all comparisons
Reads aligned to pangenome

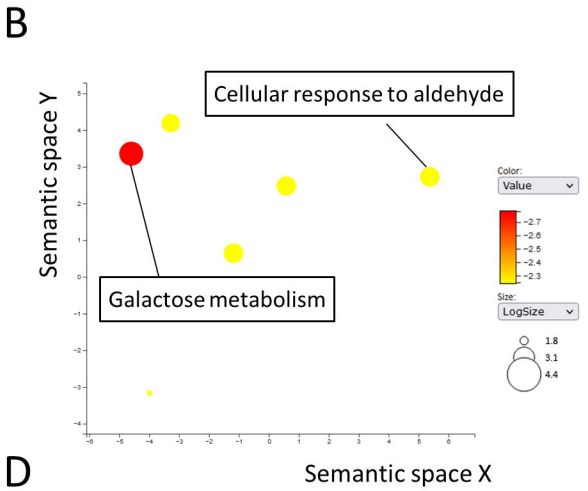
B
Cellular response to aldehyde
Galactose metabolism
Semantic space Y
Semantic space X

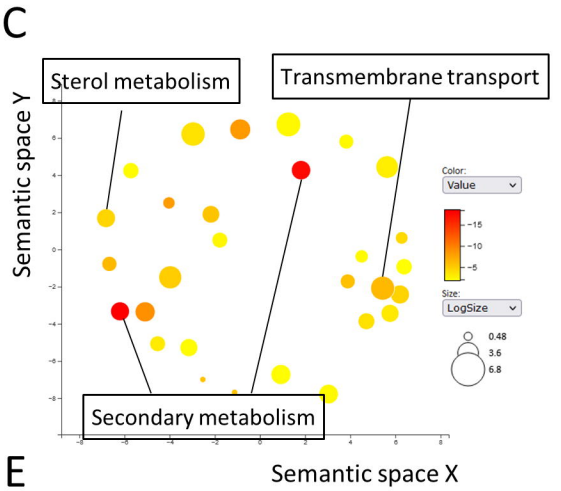
C
Sterol metabolism
Transmembrane transport
Secondary metabolism
Semantic space Y
Semantic space X

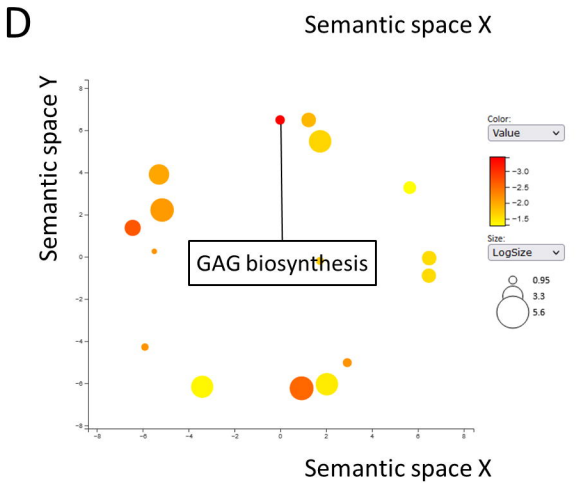
D
GAG biosynthesis
Semantic space Y
Semantic space X

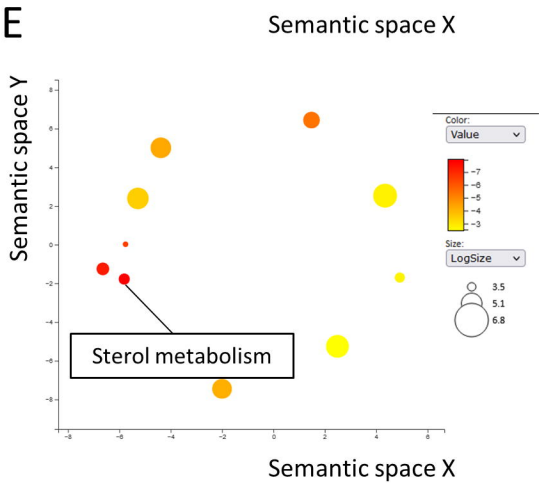
E
Sterol metabolism
Semantic space Y
Semantic space X

Fig. 5

A

Voriconazole		
Isolate	MIC	MIC +GAG
ATCC	0.5-1	0.5-1
PD-9	0.5-1	0.5-1
PD-104	0.5-1	0.5-1
PD-60	0.5-1	0.5-1

B

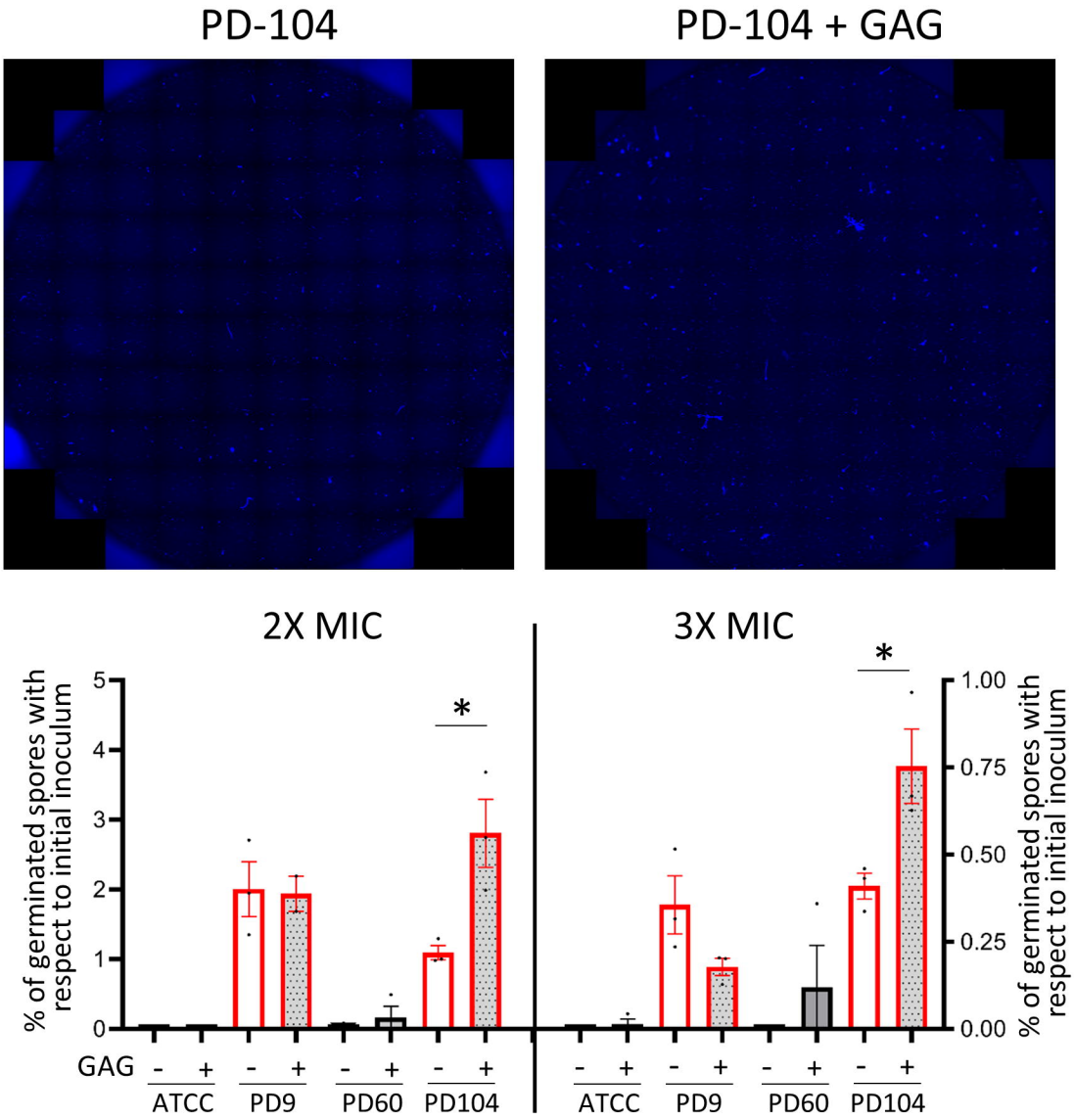

C

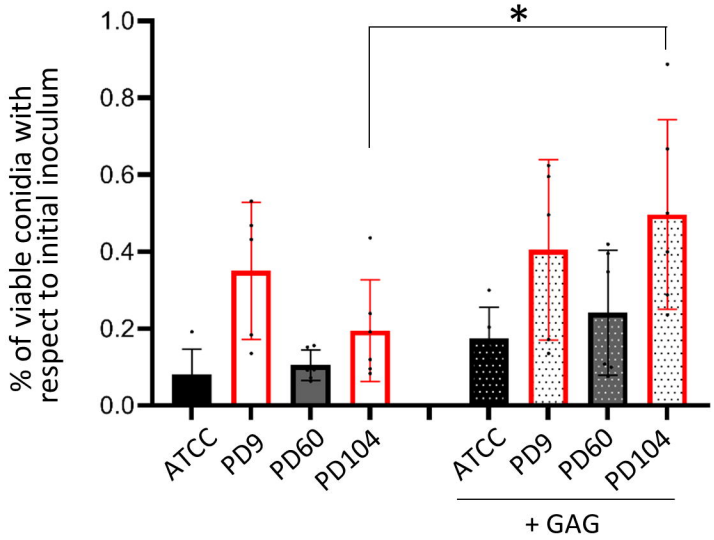

Fig. 6

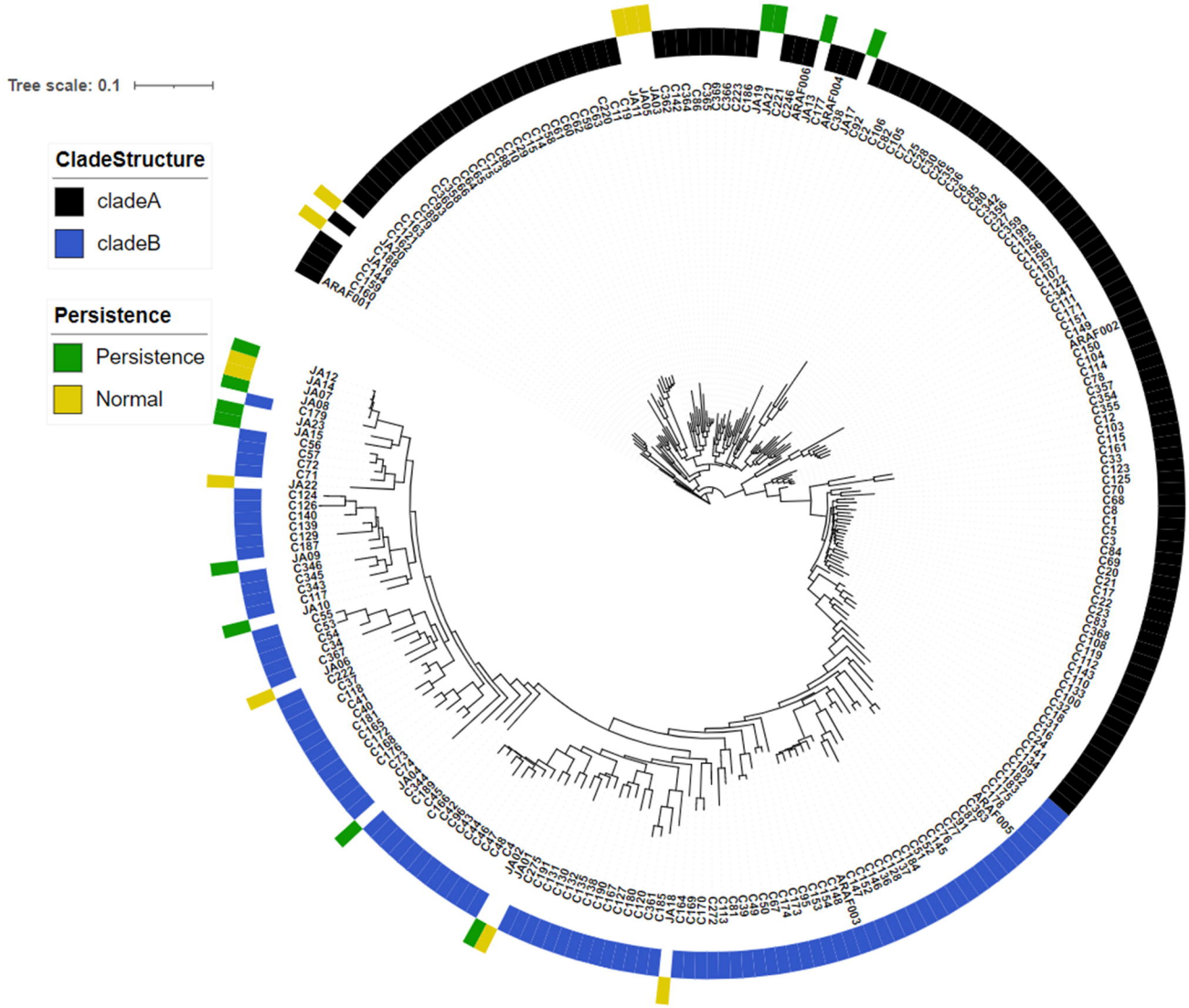
Tree scale: 0.1
CladeStructure
cladeA
cladeB
Persistence
Persistence
Normal

Fig. 7

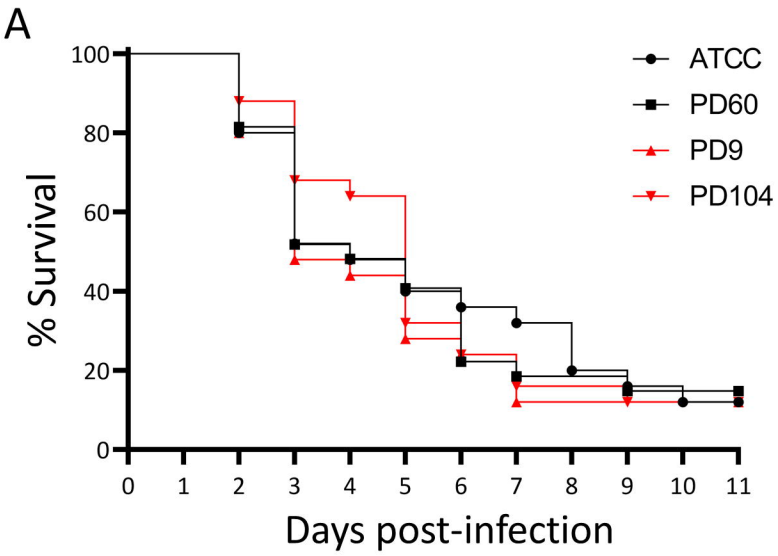
A
% Survival
Days post-infection
ATCC
PD60
PD9
PD104
0
20
40
60
80
100
0 1 2 3 4 5 6 7 8 9 10 11

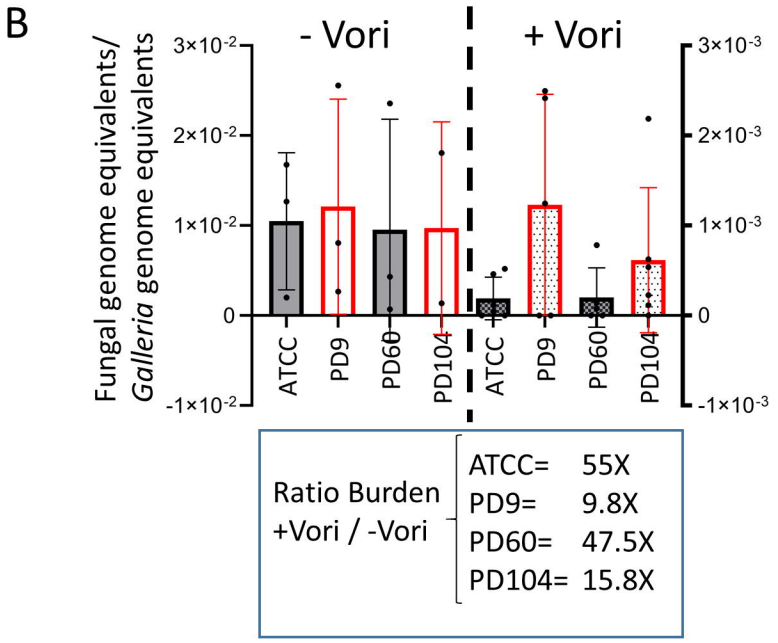
B
Fungal genome equivalents/
Galleria genome equivalents
- Vori
+ Vori
3×10-2
2×10-2
1×10-2
0
-1×10-2
3×10-3
2×10-3
1×10-3
0
-1×10-3
ATCC
PD9
PD60
PD104
ATCC
PD9
PD60
PD104
Ratio Burden
+Vori / -Vori
ATCC= 55X
PD9= 9.8X
PD60= 47.5X
PD104= 15.8X